Aging Cell

WILEY

RESEARCH ARTICLE OPEN ACCESS

Rapamycin Exerts Its Geroprotective Effects in the Ageing Human Immune System by Enhancing Resilience Against DNA Damage

Loren Kell[1,2,3] | Eleanor J. Jones[4,5] | Nima Gharahdaghi[4,6] | Daniel J. Wilkinson[4] | Kenneth Smith[4] | Philip J. Atherton[4,7] | Anna K. Simon[3,8] | Lynne S. Cox[1] | Ghada Alsaleh[2,3]

[1]Department of Biochemistry, University of Oxford, Oxford, UK | [2]Botnar Institute for Musculoskeletal Sciences, Nuffield Department of Orthopaedics, Rheumatology and Musculoskeletal Sciences (NDORMS), University of Oxford, Oxford, UK | [3]The Kennedy Institute of Rheumatology, Nuffield Department of Orthopaedics, Rheumatology and Musculoskeletal Sciences (NDORMS), University of Oxford, Oxford, UK | [4]MRC-Versus Arthritis Centre for Musculoskeletal Ageing Research, Centre of Metabolism, Ageing and Physiology (COMAP), Academic Unit of Injury, Recovery and Inflammation Sciences (IRIS), School of Medicine, University of Nottingham, Royal Derby Hospital, Derby, UK | [5]School of Sport, Exercise and Health Sciences, Loughborough University, Loughborough, UK | [6]Centre for Human Genetics (CHG), University of Oxford, Oxford, UK | [7]Ritsumeikan University, Kyoto, Japan | [8]Max Delbrück Center for Molecular Medicine, Berlin, Germany

Correspondence: Ghada Alsaleh (ghada.alsaleh@ndorms.ox.ac.uk) | Philip J. Atherton (philip.atherton@nottingham.ac.uk) | Anna K. Simon (katja.simon@mdc-berlin.de) | Lynne S. Cox (lynne.cox@bioch.ox.ac.uk)

Received: 25 September 2025 | **Revised:** 19 December 2025 | **Accepted:** 24 December 2025

Keywords: ageing | cell senescence | DNA damage | genome stability | immunosenescence | mTOR | rapamycin

ABSTRACT

mTOR inhibitors such as rapamycin are among the most robust life-extending interventions known, yet the mechanisms underlying their geroprotective effects in humans remain incompletely understood. At non-immunosuppressive doses, these drugs are senomorphic, that is, they mitigate cellular senescence, but whether they protect genome stability itself has been unclear. Given that DNA damage is a major driver of immune ageing, and immune decline accelerates whole-organism ageing, we tested whether mTOR inhibition enhances genome stability. In human T cells exposed to acute genotoxic stress, we found that rapamycin and other mTOR inhibitors suppressed senescence not by slowing protein synthesis, halting cell division, or stimulating autophagy, but by directly reducing DNA lesional burden and improving cell survival. Ex vivo analysis of aged immune cells from healthy donors revealed a stark enrichment of markers for DNA damage, senescence, and mTORC hyperactivation, suggesting that human immune ageing may be amenable to intervention by low-dose mTOR inhibition. To test this in vivo, we conducted a placebo-controlled experimental medicine study in older adults administered with low-dose rapamycin. p21, a marker of DNA damage-induced senescence, was significantly reduced in immune cells from the rapamycin compared to placebo group. These findings reveal a previously unrecognised role for mTOR inhibition: direct genoprotection. This mechanism may help explain rapamycin's exceptional geroprotective profile and opens new avenues for its use in contexts where genome instability drives pathology, ranging from healthy ageing, clinical radiation exposure and even the hazards of cosmic radiation in space travel.

1 | Introduction

Rapamycin and other mTOR inhibitors used at low doses increase lifespan in all species tested to date (Bjedov et al. 2010; Ha and Huh 2011; Harrison et al. 2009). Importantly, this lifespan extension corresponds with increased healthspan, as rapamycin has been shown to improve health across multiple domains (Wilkinson et al. 2012). Further gains in lifespan

extension have been reported when rapamycin is administered in combination with other geroprotectors such as trametinib (Gkioni et al. 2025). Though mTOR inhibitors have shown remarkable anti-ageing potential, the exact hallmarks of ageing on which they impact are not fully understood (Weichhart 2018). One explanation is that mTOR inhibitors such as rapamycin are senomorphic, in that they limit cellular senescence, a physiological process by which highly damaged cells exit the cell cycle and assume a pro-inflammatory, tissue-remodelling phenotype (Walters et al. 2016; Rolt et al. 2019; Park et al. 2020; Walters and Cox 2018). mTOR activity increases during the in vitro senescence of primary human fibroblasts and in human muscle ageing in vivo (Walters et al. 2016; Carroll et al. 2017; Markofski et al. 2015). Further to this correlative data, cells with constitutive mTOR activation enter premature replicative cell senescence in vitro, suggesting mTOR hyperactivity is sufficient to drive cellular ageing (Zhang et al. 2003). Consistent with a role of mTOR in ageing and senescence, mTOR inhibitors attenuate a variety of senescence phenotypes and extend replicative lifespan in vitro (Walters et al. 2016; Rolt et al. 2019; Park et al. 2020). In aged mice, haematopoietic stem cells show mTOR hyperactivation and transcriptional upregulation of senescence markers $p16^{Ink4a}$ (hereafter, p16) and $p19^{Arf}$, which are both decreased by rapamycin treatment in vivo (Chen et al. 2009). In humans, rapamycin reduced the presence of dermal cells expressing p16 when administered in a topical skin cream (Chung et al. 2019). The primary cellular mechanisms underlying these senomorphic properties of mTOR inhibitors are not fully understood, though impacts on slowing protein synthesis, the cell cycle, or supporting the removal of dysfunctional organelles and protein aggregates through enhanced autophagy have been suggested (Weichhart 2018). Furthermore, there is a gap in our understanding of how mTOR activity is associated with the ageing of cells which drive the ageing process—namely, those of the human immune system, for which there is increasing evidence that DNA damage is a key driver (Kell et al. 2023).

Recent studies have demonstrated how ageing of the immune system (immunosenescence) can precipitate whole-organism ageing (Yousefzadeh, Flores, et al. 2021; Desdin-Mico et al. 2020), highlighting how strategies which target immunosenescence are at the frontiers of geriatric medicine. Since aged T cells drive tissue destruction and multimorbidity during ageing, they further provide a cellular target for therapeutic anti-ageing intervention (Soto-Heredero et al. 2023; Koufaris et al. 2025). At high doses, rapamycin is immunosuppressive and causes side effects such as poor wound healing, ulcers, and loss of metabolic control leading to diabetes (Knight et al. 2007; Altomare et al. 2006; Houde et al. 2010). On the other hand, at low doses, mTOR inhibition is one of the few interventions which has been shown actually to improve immunity in older people—that is, to attenuate immunosenescence (Mannick and Lamming 2023). In humans, low-dose mTOR inhibitor RAD001 (everolimus) improved B and T cell responses to influenza vaccination in older adults (Mannick et al. 2018; Mannick et al. 2014). A second generation mTOR inhibitor RTB101 significantly reduced respiratory tract infections (RTIs) in older adults in a Phase 2b clinical trial in 652 study participants (Mannick et al. 2021). While a larger Phase 3 trial did not reach significance for reduction in mild RTIs, there was a clear trend to improved immune function (Mannick et al. 2021). mTOR inhibitors therefore offer a therapeutic route to enhance ageing immune responses against viral pathogens for which we currently lack effective pharmacological interventions. However, there is a gap in our understanding of how they impact on cellular processes such as immune cell ageing, which underpins immunosenescence and subsequent organismal ageing, in an immune-unchallenged steady state.

There is accumulating evidence that DNA damage is a central driver of immune cell ageing, immunosenescence, and whole-organism ageing (Kell et al. 2023; Yousefzadeh, Henpita, et al. 2021; Yousefzadeh, Flores, et al. 2021; Koufaris et al. 2025). In this study, we aimed to determine whether low-dose mTOR inhibition could enhance DNA stability in human T cells, a key immune cell type affected by age-related DNA damage. Using a combination of in vitro DNA damage assays, ex vivo profiling of age-related immune cells and an in vivo intervention with rapamycin in older people, we sought to explore mTOR inhibitors as a potential strategy to protect cells from DNA damage and limit senescence. Our findings have implications for geriatric medicine, radioprotection during cancer therapy and safeguarding astronauts from cosmic radiation.

2 | Results

2.1 | DNA Damage in T Cells Is Associated With Elevated mTORC Signalling

In order to develop an in vitro model for DNA damage and a reliable read-out in primary human immune cells, we cultured isolated human peripheral blood mononuclear cells (PBMCs) from healthy donors with T cell activating antibodies against CD3 and CD28 for 3 days, followed by treatment with zeocin, a double-strand break (DSB) inducer, for 2 h (DSBs in circulating leukocytes are predictive of increased mortality in humans (Bonassi et al. 2021)). Acute 15-min exposure to hydrogen peroxide was used as a positive control for DNA damage induction (Figure 1a). After recovery, cells were analysed by flow cytometry to identify $CD4^+$ and $CD8^+$ T cells, and assessed for levels of the DNA damage marker, γH2AX (gating strategy in Figure S1).

As seen in Figure 1b, zeocin treatment led to a marked increase in T cells positive for γH2AX, with a similar though more extensive shift to γH2AX-positivity in the peroxide-treated controls. This increased γH2AX signal was associated with a large increase in the percentage of T cells staining positive for γH2AX, from ~10% untreated control cells to ~30% zeocin-treated both $CD4^+$ and $CD8^+$ cells (Figure 1c). We note that the small percentage of the untreated control cells showing γH2AX positivity potentially indicates DSB formation during activation. Levels of γH2AX positivity peaked at 4 h post zeocin treatment, reducing by 24 h of recovery (Figure 1d). Consistent with elevated γH2AX, zeocin-treated cells also showed elevated DNA damage response signalling, including phosphorylation of checkpoint kinases Chk1 and Chk2, as well as increased protein levels of tumour suppressor p53, which is stabilised by phosphorylation during the DDR, and its transcriptional target, the cyclin-kinase inhibitor p21 (Figure 1e). To determine whether DNA damage correlates with changes in mTOR activity, we further analysed

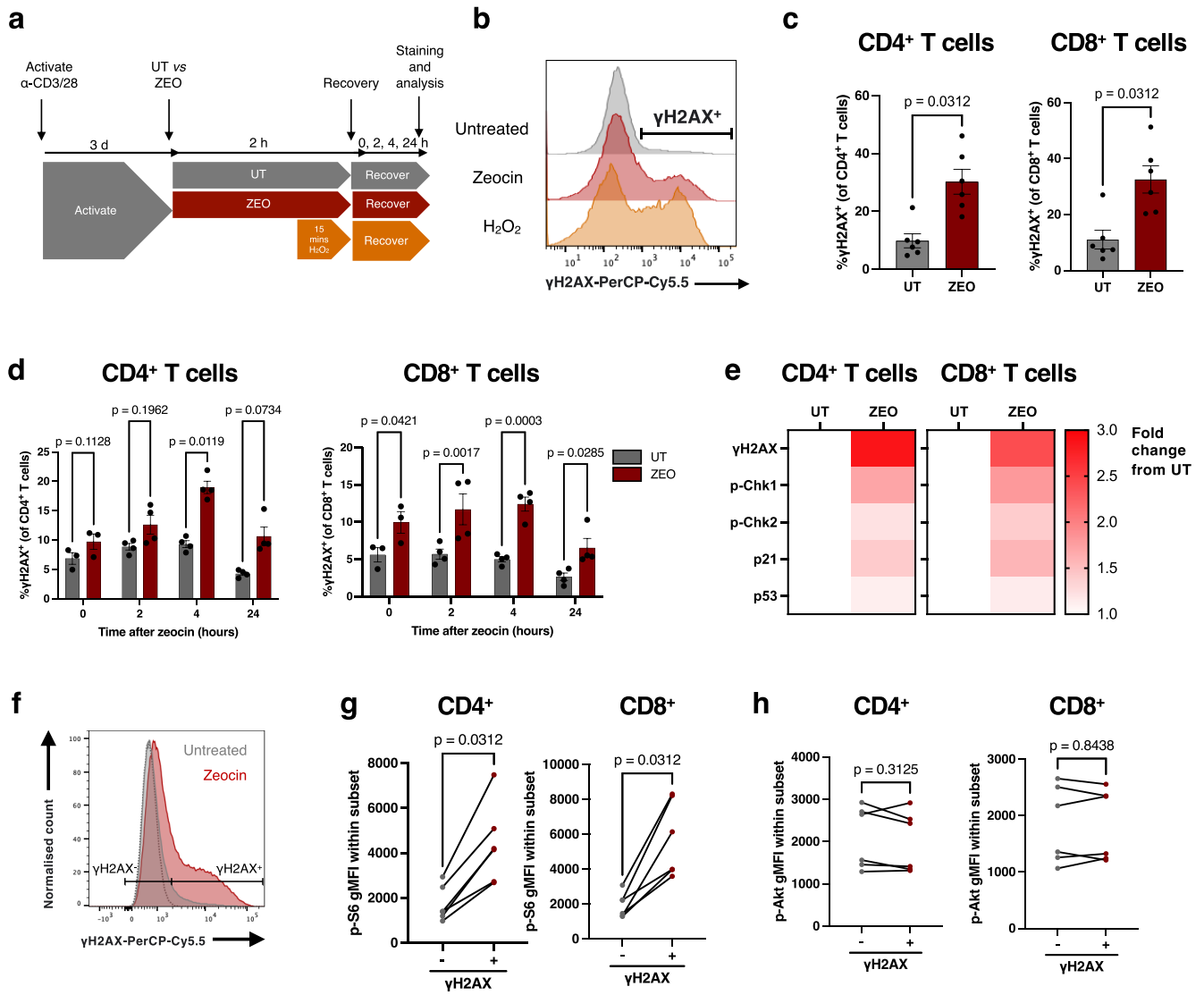

FIGURE 1 | T cell DNA damage is associated with elevated mTORC1 activity. (a) DNA damage assay design. (b) Representative histograms of γH2AX levels by flow cytometry following 4-h recovery in untreated, zeocin-treated (200 μg/mL) and H_2O_2-treated (25 μM) PBMCs gated on $CD4^+$ T cells. (c, d) Proportion of $\gamma H2AX^+$ of $CD4^+$ (left) and $CD8^+$ (right) T cells after (c) 4 h recovery from zeocin treatment, $n = 6$ healthy donors or (d) across different recovery times after zeocin treatment, from 4 independent experiments using PBMCs from 1 donor. (e) Heatmaps for levels of DDR signalling molecules expressed as fold change from untreated (UT) cells. (f) Representative gating of $\gamma H2AX^+$ and $\gamma H2AX^-$ cells based on untreated (grey), zeocin-treated (red) cells, and fluorescence minus one (FMO, dotted grey) control. (g, h) Geometric mean fluorescence intensity (gMFI) of (g) p-S6 and (h) p-Akt in zeocin-treated $CD4^+$ or $CD8^+$ T cells gated as either positive or negative for γH2AX, $n = 6$ healthy donors. *p*-values are derived from a two-way ANOVA with Šídák's multiple comparisons test (d), and a Wilcoxon matched-pairs signed rank test (c, g, h).

T cells with low and high levels of γH2AX for their level of phosphorylated mTORC1 target S6 (p-S6) and mTORC2 target Akt (p-Akt) (Figure 1f). Notably, both $CD4^+$ and $CD8^+$ cells with high γH2AX signals showed significant increases in phosphorylated S6 (Figure 1g), an indirect target of mTORC1, but no change in levels of in mTORC2 target p-Akt (Figure 1h), suggesting that DNA damage in T cells is associated with elevated mTORC1 activity.

2.2 | Suppression of mTORC Signalling Reduces Markers of DNA Damage in Human T Cells In Vitro

To test the association between high levels of DNA damage markers and elevated mTORC signalling, we assessed the impact of mTORC inhibitors on the DDR in the zeocin-induced DNA damage model. T cells were incubated throughout their 3-day activation, 2-h zeocin treatment, and 4-h recovery periods with low dose mTORC1 inhibitor rapamycin (10 nM), pan-mTOR inhibitor AZD8055 (100 nM) or DMSO vehicle control (Figure 2a). Exposure to rapamycin and AZD8055 over this 3-day activation significantly suppressed p-S6 levels, apparent at as early as 6 h (Figure S2a,b). CD25 upregulation, a marker of T cell activation, was not impacted by mTOR inhibition at this low dose (Figure S2c). As before (Figure 1b,c), zeocin treatment resulted in a significant increase in overall γH2AX levels. However, this surge in γH2AX was greatly attenuated by treatment with the mTOR inhibitors rapamycin or AZD8055 (Figure 2b), reflected by the percentage of $CD4^+$ T cells staining positive for γH2AX after zeocin treatment being significantly reduced by both

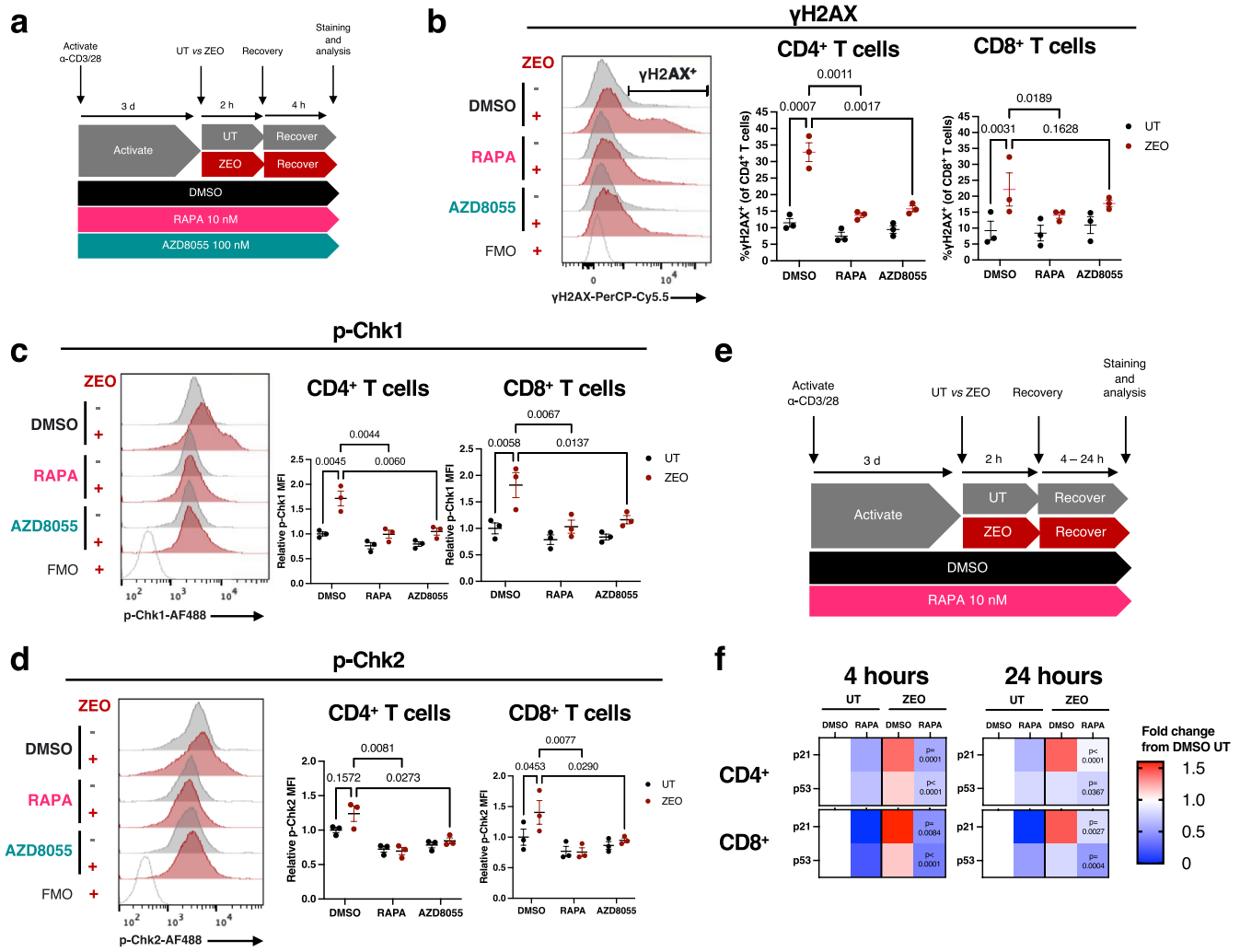

FIGURE 2 | mTOR inhibition reduces the DNA damage response in genotoxin-exposed human T cells from healthy donors. (a) Experimental design. (b) Representative flow cytometry fluorescence histograms of γH2AX levels in CD4⁺ T cells with fluorescence minus one (FMO) control (left), with quantification of the proportion of γH2AX⁺ cells across conditions in CD4⁺ and CD8⁺ T cells, $n = 3$ healthy donors. (c, d) Representative fluorescence histograms of p-Chk1 (c) or p-Chk2 (d) levels in CD4⁺ T cells, with quantification of fluorescence relative to average of DMSO untreated control in CD4⁺ and CD8⁺ T cells, $n = 3$ healthy donors. (e) Experimental design for (f). (f) Heatmaps of gMFI of p21 and p53 assessed by flow cytometry, in CD4⁺ and CD8⁺ T cells at 4 and 24 h recovery from zeocin, expressed as fold change from the DMSO untreated (UT) condition for each recovery time point. *p*-values represent comparisons to the DMSO zeocin (ZEO) condition, $n = 4$ healthy donors. *p*-values are determined from a two-way ANOVA with Šídák's (b–d) or Dunnett's (f) multiple comparisons test.

mTOR inhibitors (Figure 2b, middle). By contrast, in CD8⁺ cells, this reduction was only significant on rapamycin treatment (Figure 2b, right).

To investigate further whether mTOR inhibition affected signalling within the DNA damage response, we assessed levels of phosphorylated (i.e., activated) checkpoint kinases Chk1 and Chk2. Both rapamycin and AZD8055 treatment prevented the zeocin-induced increase in levels for both p-Chk1 and p-Chk2 in both CD4⁺ and CD8⁺ cells (Figure 2c,d). We additionally assessed levels of the DDR proteins p53 and p21 at both 4 h recovery from zeocin, and at a later 24-h timepoint, to assess longer-term effects on resolution of the DDR (Figure 2e). Notably, in control cells without zeocin-induced DNA damage, rapamycin treatment led to reduction in p53 and p21 levels, compared with DMSO vehicle controls (Figure 2f). p21 levels increased by 4 h recovery following zeocin treatment, remaining elevated at 24 h; this response was completely ablated on mTOR inhibition by rapamycin treatment (Figure 2f). Similarly, the elevated p53 signal seen at 4 h was significantly reduced on rapamycin treatment. By 24 h, the p53 signal was reduced in zeocin-treated cells (with and without rapamycin treatment) compared with levels at 4 h post damage in both CD4⁺ and CD8⁺ T cells, though mTORC inhibition led to a further significant drop in p53 levels (Figure 2f).

2.3 | Direct Association Between High Levels of Damage and Elevated mTORC Signalling

Having identified that continuous mTOR inhibition suppressed DDR upregulation, we next investigated the temporal nature of this effect by incubating cells with rapamycin either before, during, or after DNA damage by zeocin exposure (Figure 3a). To do this, T cells within PBMC cultures from

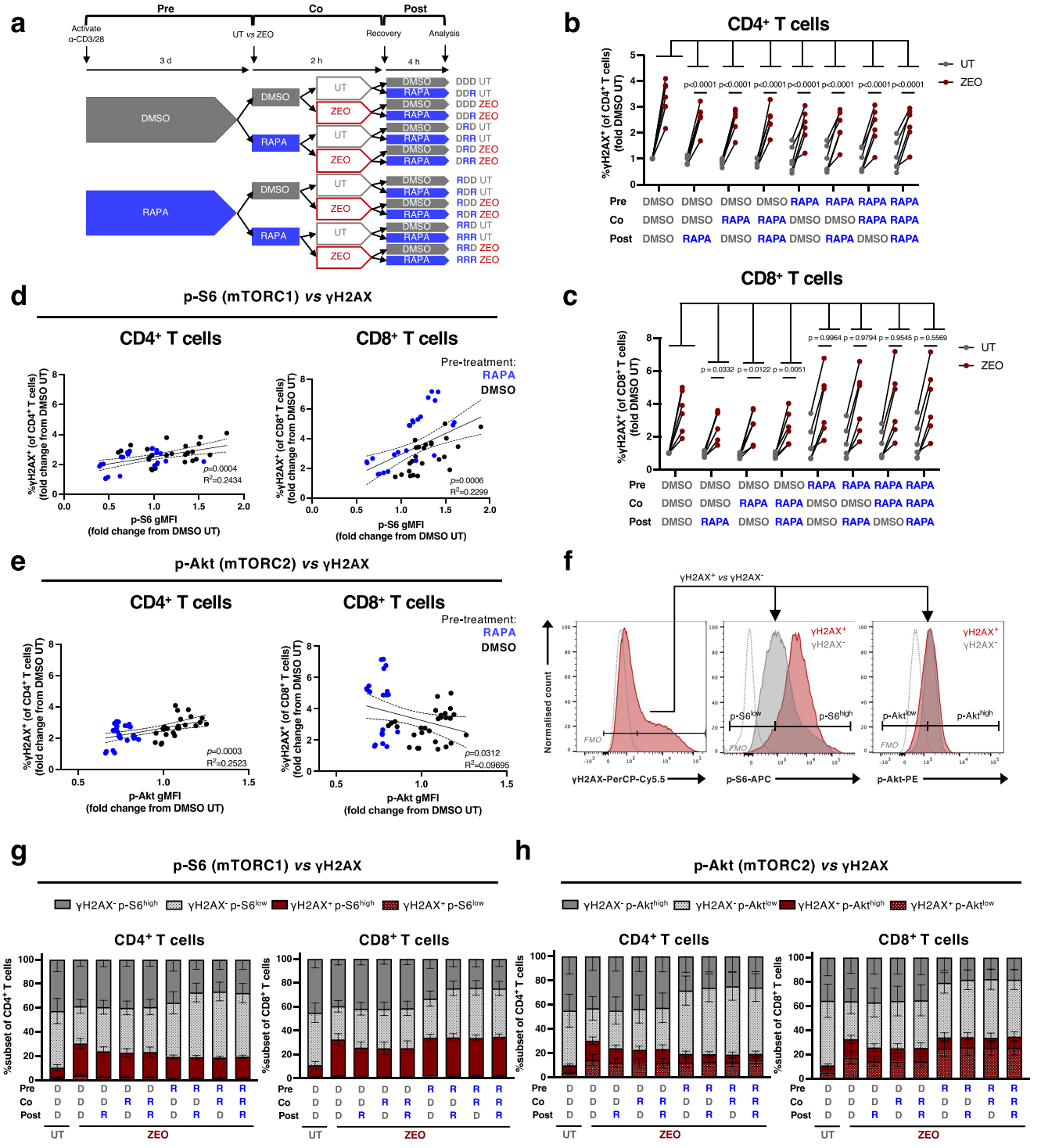

FIGURE 3 | Rapamycin inhibits γH2AX at any point with respect to genotoxic treatment and suppression of mTOR activity correlates with DNA damage. (a) Experimental design. (b, c) Proportion of γH2AX$^+$ of (b) CD4$^+$ and (c) CD8$^+$ T cells, in PBMCs treated with 10 nM RAPA or DMSO vehicle control pre-, co-, and/or post-treatment with zeocin. Each data point is represented as fold change in γH2AX$^+$ cells from DMSO → DMSO → DMSO untreated (UT) cells on a per-donor basis. *p*-values represent comparisons between the DMSO→DMSO→DMSO zeocin (ZEO) condition and all other zeocin treatment conditions that included rapamycin, $n = 6$ healthy donors. (d, e) Simple linear regression analyses from experiment in (a), of γH2AX and either p-S6 (d) or p-Akt (e) in zeocin-treated CD4$^+$ or CD8$^+$ T cells. Values are expressed as fold change from DMSO → DMSO → DMSO UT with line of best fit and 95% confidence intervals indicated. Data are pooled from 6 independent experiments, $n = 6$ healthy donors. (f) Representative gating of p-S6^{high}, p-S6^{low}, p-Akt^{high} and p-Akt^{low} populations within γH2AX$^+$ (red) and γH2AX$^-$ (grey) zeocin-treated CD4$^+$ T cells, based on fluorescence minus one (FMO, dotted grey) controls. (g, h) Quantification of populations gated as in (f) across conditions in (a) for (g) p-S6 and (h) p-Akt levels, $n = 6$ healthy donors. *p*-values are derived from a two-way ANOVA with Šídák's (b, c) multiple comparisons test.

healthy donors were activated for 3 days with anti-CD3 and anti-CD28 antibodies, then sequentially split into aliquots and incubated with rapamycin or DMSO ± zeocin as shown in Figure 3a. Following the recovery period also in the presence or absence of rapamycin, the percentage of cells staining positive for the DNA damage marker γH2AX was assessed by flow cytometry. In all cases, zeocin treatment resulted in an increase in γH2AX-positive cells (Figure 3b,c), but $CD4^+$ T cells showed a significant reduction of γH2AX positivity when treated with rapamycin before, during, or after zeocin treatment compared with the DMSO-only controls with zeocin (Figure 3b). Furthermore, the fold increase in $γH2AX^+$ cells significantly correlated with levels of both p-S6 and p-Akt, consistent with a role for mTOR activity in a highly DNA-damaged phenotype (Figure 3d,e). The exception to this was p-Akt in $CD8^+$ T cells, which negatively correlated with levels of γH2AX (Figure 3e, right), consistent with the result that treatment with rapamycin only during or after zeocin treatment (at times when p-Akt was not suppressed) could minimise γH2AX induction (Figure 3c). Next, we assessed the proportion of cells gated as $p\text{-}S6^{high}$, $p\text{-}S6^{low}$, $p\text{-}Akt^{high}$ and $p\text{-}Akt^{low}$ within the $γH2AX^+$ and $γH2AX^-$ populations following zeocin treatment (Figure 3f). We observed that the effect of rapamycin in decreasing the proportion of cells showing high levels of $γH2AX^+$ (red bars) was accompanied by an expansion of a $γH2AX^-$ population showing low levels of p-S6 and p-Akt (dotted grey bars) (Figure 3g,h). Intriguingly, the small proportion of cells that remained positive for γH2AX following rapamycin treatment were predominantly $p\text{-}S6^{high}$ (filled red bar) and may potentially represent a population that is resistant to pharmacological mTOR inhibition (Figure 3g). In summary, these data suggest that rapamycin treatment either before, during, or after exposure to a genotoxin (i.e., even short-term treatment) could prevent zeocin-induced γH2AX levels.

2.4 | Reduction in DNA Damage Markers by mTOR Inhibition Is Not due to Impacts on Cell Cycle or Protein Synthesis

Progression through the cell cycle is halted during the initial stages of the DDR to allow for repair of DNA lesions. Thus, one possible explanation for our observation that mTOR inhibition limits $γH2AX^+$ DNA damage in T cells is that it promotes cell cycle arrest to support DNA repair. We therefore first measured the proportion of cells in each phase of the cell cycle (G_0/G_1, S or G_2/M) in untreated and zeocin-treated T cells using flow cytometry (Figure S3a). Zeocin treatment of both $CD4^+$ and $CD8^+$ T cells halved the proportion of cells in S-phase (from 52% without zeocin to 26% with zeocin treatment) with a concomitant increase in the proportion of cells in G_2/M phase (from 1.3% to 15%) (Figure S3b), suggesting that DNA-damaged cells proceed to G_2 but then activate cell cycle checkpoints to prevent cell division.

To test whether mTOR inhibition affected cell cycle progression, cells were treated with rapamycin continuously (RRR), during (DRD) and/or after treatment (DRR, DDR) with zeocin. Under these conditions previously, rapamycin limited zeocin-induced γH2AX levels in $CD4^+$ and $CD8^+$ T cells (Figure 3b,c). We observed an increase in the G_0/G_1-phase population on continuous rapamycin treatment (RRR) in cells without overt DNA damage (i.e., γH2AX negative), though it did not affect the proportion of G_0/G_1-phase cells in the γH2AX-positive population, indicating that continuous rapamycin treatment did not change cell cycle phase distribution in the context of DNA damage (Figure S3c). Since rapamycin treatment before, during, or after zeocin treatment, or continuous exposure (DDR, DRD, DRR and RRR) effectively limited the induction of γH2AX in T cells (Figure 3b,c), but did not affect cell cycle phase distribution in DNA-damaged $γH2AX^+$ cells (Figure S3c), we concluded that the effect of rapamycin on γH2AX was not due to effects on the cell cycle.

mTOR is a master anabolic regulator of protein synthesis (e.g., by activating ribosomal S6 protein through S6K-dependent phosphorylation), so it is conceivable that the reduced levels of DNA damage proteins we detect by flow cytometry may be a consequence of blockade of their *de novo* synthesis (albeit that the acute DDR is predominantly mediated post-translationally). To evaluate the effects of rapamycin on nascent protein synthesis in the DNA damage assay, cells were treated with rapamycin or DMSO vehicle control before, during and/or after zeocin treatment and then incubated for the final 30 min of their 4-h recovery from zeocin with O-propargyl-puromycin (OPP), an alkyne analogue of puromycin that is incorporated into nascent polypeptides and halts further translation (Figure S3d). The mean fluorescence of labelled OPP in cells thus reports short-term total *de novo* protein synthesis. One-hour treatment with 50 μg/mL cycloheximide (CHX) served as a positive control for inhibition of protein synthesis. As expected, CHX-treated cells incorporated significantly less OPP than the DMSO untreated controls (Figure S3e). Rapamycin treatment both during and after zeocin exposure (DRR) did not significantly affect OPP incorporation, though continuous rapamycin treatment (RRR) showed a non-significant trend towards lower OPP fluorescence (Figure S3e). Since there was no consistent effect of rapamycin in decreasing OPP levels, this suggests that the effect of rapamycin on limiting zeocin-induced DDR signalling levels was not due to decreasing global protein synthesis. In summary so far, our data indicate that the rapamycin-mediated protection from upregulation of the DDR following zeocin exposure is likely independent of effects on the cell cycle and protein synthesis.

2.5 | Autophagy Is Required to Limit DNA Damage in T Cells, but Rapamycin's Protective Effect Is Autophagy-Independent

Autophagy is a cytoprotective cell recycling process that is repressed by mTORC1 activity. Notably, autophagy is also involved in regulation of the DNA damage response (Vessoni et al. 2013). We therefore probed whether the mechanism by which rapamycin treatment reduces markers of DNA damage signalling following zeocin exposure could be due to enhancement of autophagic flux, as measured by a flow cytometry-based LC3 assay (Figure S4a,b) (Alsaleh et al. 2020). In the presence of zeocin-induced damage (Figure S5a), activated T cells with a high DNA damage load (i.e., positive for γH2AX) showed significantly lower autophagic flux than those cells negative for γH2AX (Figure S5b). This suggests either that cells bearing a

heavy DNA lesional load are less able to undergo autophagy, or that those with effective autophagy rapidly resolve DNA damage leading to low levels of damage markers such as γH2AX.

To distinguish between these possibilities, we used the drug chloroquine to inhibit autophagy, which effectively halved autophagic flux in activated T cells (Figure S4c). In zeocin-treated cells, autophagy blockade increased γH2AX-positive cells, confirming that autophagy does limit DNA damage in human T cells (Figure S5c). Next, we asked whether rapamycin enhanced autophagy in zeocin-exposed cells (Figure S5d) and found that this was the case, regardless of γH2AX levels or timing of rapamycin administration (Figure S5e). We then asked whether rapamycin's protective effect on DNA damage depended on autophagy by co-treating cells with rapamycin and chloroquine (Figure S5f). As expected, chloroquine inhibited autophagic flux and increased γH2AX positivity, but rapamycin still markedly reduced DNA damage despite strong autophagy inhibition in the context of chloroquine co-treatment (Figures S4d and S5g). These findings indicate that while autophagy supports DNA damage resolution in human T cells, rapamycin's protective effect is independent of cell cycle pausing, protein synthesis, and autophagy.

2.6 | Rapamycin Decreases Overall DNA Lesional Burden and Reduces T Cell Death Following DNA Damage

DDR signalling requires activation of several PI3-like kinases (e.g., DNA-PKcs, ATM and ATR). It is therefore possible that mTOR inhibitors reduce apparent DNA damage by inhibiting critical DDR enzyme signalling, in a manner that would be highly detrimental to cell health and survival. Alternatively, reduced levels of DDR signalling may instead reflect a lower DNA lesional burden. To distinguish between these two possibilities, we assessed the extent of DNA breaks after 4 h of recovery from zeocin exposure, using the alkaline comet assay, in isolated $CD4^+$ T cells treated with or without rapamycin (Figure 4a). Treatment with hydrogen peroxide was used as a positive control for DNA breakage. Both zeocin and hydrogen peroxide treatment significantly increased DNA lesions (both DSBs and SSBs) compared to untreated controls (Figure 4b,c). Notably, DNA lesion burden was markedly reduced in $CD4^+$ T cells treated with rapamycin at this 4-h recovery timepoint from zeocin. This suggests that the reduction in DDR signalling afforded by rapamycin is due to enhanced genome stability rather than downstream inhibition of DDR enzymes (Figure 4b,c).

To assess further the kinetics of DNA lesional burden and potential resolution of damage, we then assessed comet Olive moments in cells incubated continuously with rapamycin over a time course of up to 24 h after exposure to zeocin. The peak of DNA lesions manifesting as comet tails was found to occur at 4 h after zeocin treatment (Figure 4d). Continuous rapamycin treatment significantly limited the DNA lesion burden at all timepoints tested (Figure 4d). Notably, rapamycin reduced comet tails even at 0 h post-zeocin exposure—i.e., directly after genotoxin treatment—suggesting a stark enhancement of resilience from DNA damage that may reflect prevention of DNA lesion formation. In summary, we can rule out a negative effect of rapamycin inhibiting PI3-like kinases in the DDR, and instead propose that rapamycin positively protects cells from DNA damage.

To explore whether this effect of rapamycin on reducing lesional load has an impact on overall cell physiology, we measured cell viability by assessing fluorescence of a membrane-impermeable dye that is taken up only by dead cells (Figure 4e). Consistent with the increase in cells with major DNA lesions following zeocin exposure, we observed a decrease in the percentage of live $CD4^+$ T cells at 4 h, leading to a severe reduction to only 20% live cells by 24 h recovery from zeocin in DMSO vehicle control cells. This suggests that the high lesional burden induced by zeocin treatment is lethal to the majority of T cells (Figure 4e). Remarkably, continuous treatment with low-dose rapamycin (10 nM) supported a 3-fold greater cell survival with over 60% cells still viable 24 h after zeocin treatment (Figure 4e), strongly suggesting that rapamycin does indeed enhance DNA repair responses and may therefore act as a genoprotector.

2.7 | Age-Related Immune Subsets Show Elevated Markers of DNA Damage, Cell Senescence, and mTOR Activity

Our findings so far suggest a genoprotective role for rapamycin in the immune system, but are based on an in vitro model of acute DNA damage. In humans, immunosenescence involves the expansion of terminally differentiated immune subsets linked to dysfunction (Table 1), though their exact phenotype remains unclear. Since chronic DNA damage accumulation is a key hallmark of ageing that in immune cells contributes to whole-body ageing (Yousefzadeh, Flores, et al. 2021), we examined whether aged human immune cells show signs of DNA damage and cell senescence, and whether this correlates with their mTOR activity.

Using 27-colour spectral flow cytometry, we analysed age-related immune cell subsets from healthy donor blood, identifying TEMRA T cells ($CD4^+$ and $CD8^+$), IgD^-CD27^- (double-negative) B cells, $CD16^+CD57^+$ (within $CD56^{bright}$ and $CD56^{dim}$) NK cells, and non-classical monocytes (Figure 5a, Figure S6, Table 1). We then assessed senescence- and DNA damage-associated markers (p21, p16, p53, γH2AX) and cell size (measured by forward scatter, FSC) to determine whether these subsets were enriched for ageing biomarkers compared with their naïve counterparts (Stein et al. 1999; Passos et al. 2007; Van Deursen 2014; Tsai et al. 2021).

We observed that senescence markers were significantly enriched in age-related immune cells compared to their naïve equivalents, with each of the 6 subsets assessed showing significant elevation of at least 3/5 senescence markers (Figure 5b,c). In particular, age-related $CD4^+$ and $CD8^+$ TEMRAs, and non-classical monocytes, showed the greatest number of elevated senescence markers compared to early-differentiated cells of the same lineage (4/5 each, Figure 5c). Double-negative (DN) B cells and $CD57^+CD16^+$ (double-positive, DP) NK cells all exhibited significant upregulation of 3/5 senescence markers (Figure 5c). Notably, DNA damage marker γH2AX was elevated only in age-associated T and B cells, which are immune cell types that

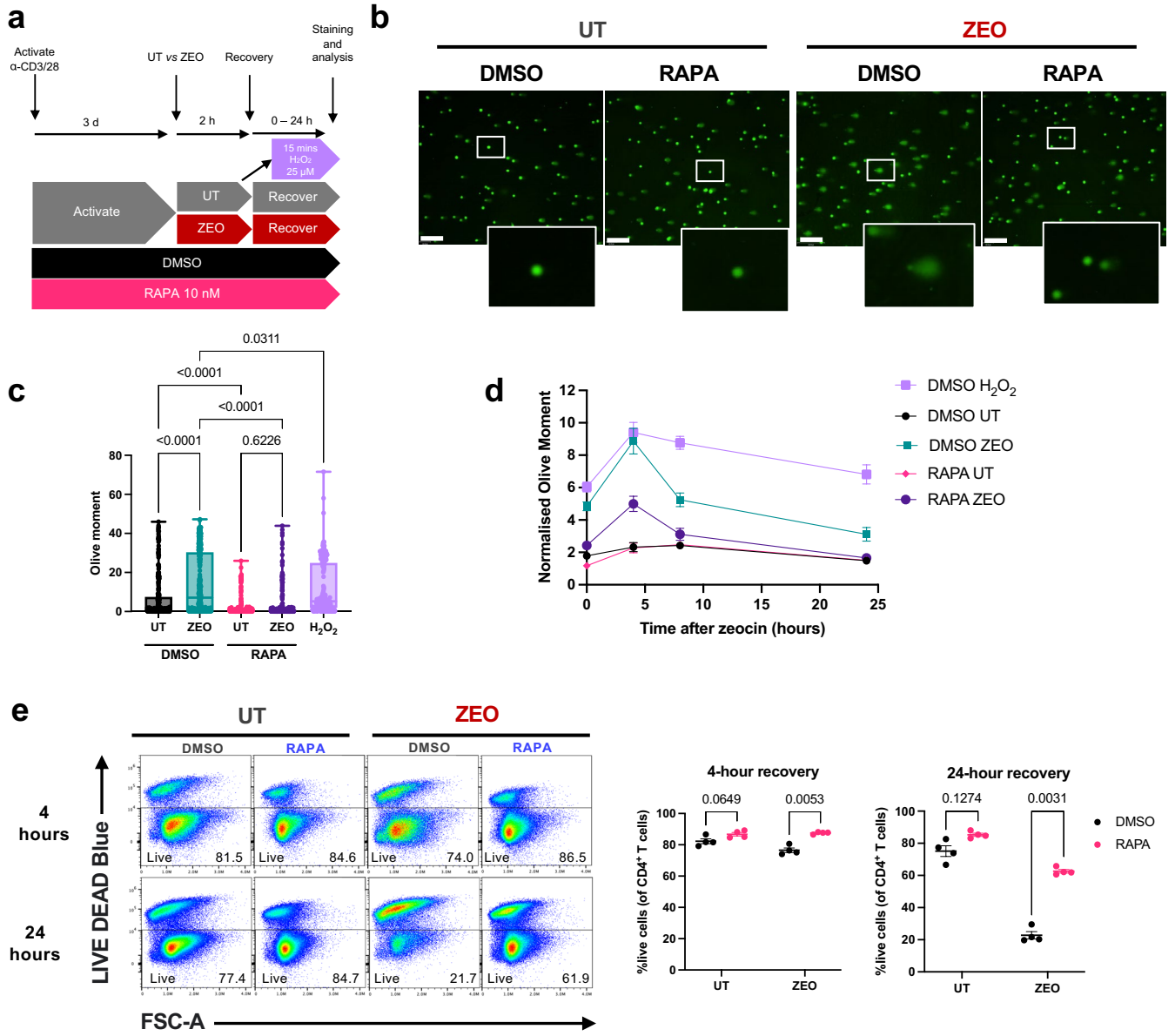

FIGURE 4 | Rapamycin attenuates DNA lesional burden and improves survival after exposure to a DNA-damaging agent. (a) Experimental design for 2-h zeocin treatment (200 µg/mL) following continuous exposure to rapamycin (10 nM) or DMSO vehicle control in isolated CD4$^+$ T cells. Treatment of cells with 25 µM H_2O_2 for 15 min served as a positive control for severe DNA damage. (b) Representative images of comets; scalebar represents 200 µm. (c) DNA lesions as measured by the Olive moment of > 250 comets analysed across conditions following a 4-h recovery from zeocin. (d) Comet Olive moments throughout a 24-h time course of recovery from zeocin normalised to the median value of the DMSO untreated (UT) condition at each time point. Data are the median ± SEM of 100–250 nuclei analysed per condition. Representative of three independent experiments, $n = 3$ healthy donors. (e) Live cells across conditions, as measured by lack of fluorescence of a membrane-permeable dye, at 4- and 24h recovery from zeocin exposure. *p*-values are derived from a one-way ANOVA with Tukey's multiple comparisons test (c), or a two-way ANOVA with Šídák's multiple comparisons test (e).

undergo double-strand breaks during V(D)J recombination to form T cell and B cell receptors (Figure 5b,c). Intriguingly, the most common senescence feature that was increased across age-related subsets was p21, present in all 6 age-related subsets compared to their early-differentiated controls (Figure 5c). This was followed by high p53, p16 and cell size, which were each significantly elevated in 5/6 subsets (Figure 5c). Overall, these data suggest that age-related subsets display several features of cellular senescence, and particularly overexpress the p21 and p53 pathway, suggesting a DNA-damage induced senescence phenotype. Importantly, these data demonstrate that age-related immune cells may be targetable with genoprotective senotherapeutics.

Next, we asked whether these age-related subsets showed changes in their activation of mTORC1 and mTORC2 by measuring their levels of p-S6 and p-Akt respectively. We observed that age-related CD4$^+$ TEMRAs, CD8$^+$ TEMRAs, and non-classical monocytes all showed elevated p-S6, with CD4$^+$ TEMRAs and non-classical monocytes additionally displaying increased p-Akt levels (Figure 5b,c). These findings indicate that while senescence markers were present in all age-related

TABLE 1 | Identification of age-related peripheral immune subsets in humans.

Peripheral immune cell	Age-related subset	Evidence that subset accumulates with chronological age in humans	Flow cytometry gating strategy in human blood
$CD4^+$ T cell	TEMRA, $CD27^-CD45RA^+$	(Callender et al. 2020; Libri et al. 2011; Ligotti et al. 2023)	$CD3^+CD19^-CD4^+CD8^-CD27^-CD45RA^+$
$CD8^+$ T cell	TEMRA, $CD27^-CD45RA^+$	(Callender et al. 2020; Czesnikiewicz-Guzik et al. 2008; Riddell et al. 2015; Ligotti et al. 2023)	$CD3^+CD19^-CD4^-CD8^+CD27^-CD45RA^+$
B cell	Double negative (DN), IgD^-CD27^-	(Frasca et al. 2017; Colonna-Romano et al. 2009; Nevalainen et al. 2019)	$CD3^-CD19^+CD27^-IgD^-$
NK $CD56^{bright}$	Double positive (DP), $CD16^+CD57^+$	(Hazeldine et al. 2012; Lopez-Verges et al. 2010)	$CD3^-CD19^-$HLA-DR^-CD56^+ $CD56^{bright}CD16^+CD57^+$
NK $CD56^{dim}$	Double positive (DP), $CD16^+CD57^+$		$CD3^-CD19^-$HLA-DR^-CD56^+ $CD56^{dim}CD16^+CD57^+$
Monocyte	Non-classical (NC), $CD14^-CD16^+$	(Hearps et al. 2012; Nyugen et al. 2010; Seidler et al. 2010)	$CD3^-CD19^-$HLA-$DR^+CD14^-CD16^+$

immune subsets, mTOR hyperactivation may occur only in T cell and monocyte ageing.

Given that diverse age-related subsets within healthy donors showed elevated senescence and mTORC1/2 markers, we next asked whether immune cells from older people (56–69 years old, $n=9$) exhibited increased mTORC activation compared to those from younger donors (<50 years old, $n=8$). We first verified that, compared to the younger group, older donors had an increased percentage of $CD8^+$ T cells expressing CD57 and KLRG1, and loss of expression of CD28 (Figure 5d), all of which are established markers of immunosenescence (Kell et al. 2023). Comparison of immune subsets between these two groups showed that, in addition to these markers of T cell senescence, immune ageing corresponded with an increase in p-S6 levels across all immune cell types analysed (Figure 5e). This suggests that mTORC1 activity is a broad biomarker of human immune ageing shared by cell types from diverse lineages.

2.8 | Low-Dose Rapamycin Reduces Markers of Senescence and DNA Damage in Humans In Vivo

Taken together, our data so far show that age-related immune subsets exhibit features of DNA damage, cell senescence, and mTOR hyperactivation, and that human ageing is accompanied by increased mTOR activity across all immune cell types (Figure 5d,e). We have further demonstrated that treatment with low-dose mTOR inhibitors improves survival and reduces markers of senescence and DNA damage in human T cells treated with a genotoxic agent outside of the body. Such findings are important but require in vivo data before they support further clinical action. We therefore assessed whether rapamycin treatment impacts on immune cell DNA damage and senescence in vivo in humans, analysing PBMCs from older male volunteers who received either 1 mg/day rapamycin ($n=4$) or placebo ($n=5$) for 4 months (Figure 6a). We aimed to assess whether features of immunosenescence were modulated by rapamycin in PBMCs isolated at several timepoints throughout the study.

Participants in the rapamycin and placebo groups were well-matched for age and BMI (Table 2). After 8 weeks of intervention, the concentration of rapamycin in the blood reached an average of 3.24 ± 1.81 nM in the treatment group (Figure S7a), that is, within the same order of magnitude as the doses used in our in vitro experiments (10 nM). To address concerns of immunosuppression by rapamycin, white blood cell counts were assessed at 8 weeks; there were no significant differences in leukocyte counts in the blood over the initial 8-week treatment period in either rapamycin or placebo groups, suggesting that this low-dose rapamycin treatment regimen was not immunosuppressive (Figure S7b). To assess whether mTOR activity was inhibited at this dose of rapamycin, we analysed p-S6 levels across immune subsets. We observed a significant decrease in p-S6 levels in most immune subsets in the rapamycin-treated participants compared to those in the placebo group at 4–5 weeks, suggesting successful inhibition of mTORC1 (Figure 6d). Taken together, low-dose rapamycin treatment led to detectable stable blood rapamycin concentrations at a level well below that used therapeutically for immunosuppression with no evidence of leukocyte suppression, plus reduced markers of mTORC1 activity in peripheral immune cells after 4–5 weeks.

To determine whether features of immunosenescence were impacted by in vivo rapamycin treatment, we analysed PBMCs from the study using 27-colour spectral flow cytometry (Figure S6). Simple linear regression analyses in circulating $CD4^+$ T cells revealed a strong and highly significant positive correlation between p-S6 and γH2AX levels in both treatment groups ($R^2=0.5481$ [placebo], 0.7758 [rapamycin], $p<0.0001$ in both groups), indicating that mTOR activity and DNA damage are positively linked in vivo (Figure 6b,c). Notably, T cells from the rapamycin group had lower p-S6 levels than those from the placebo group, which corresponded with decreased γH2AX levels (Figure 6c). Overall, rapamycin treatment led to a trend towards lower γH2AX levels in immune subsets, particularly in age-related CD4 TEMRA and double-negative B cells, which with higher participant numbers might show significance (Figure S7c). Consistent with these positive effects on

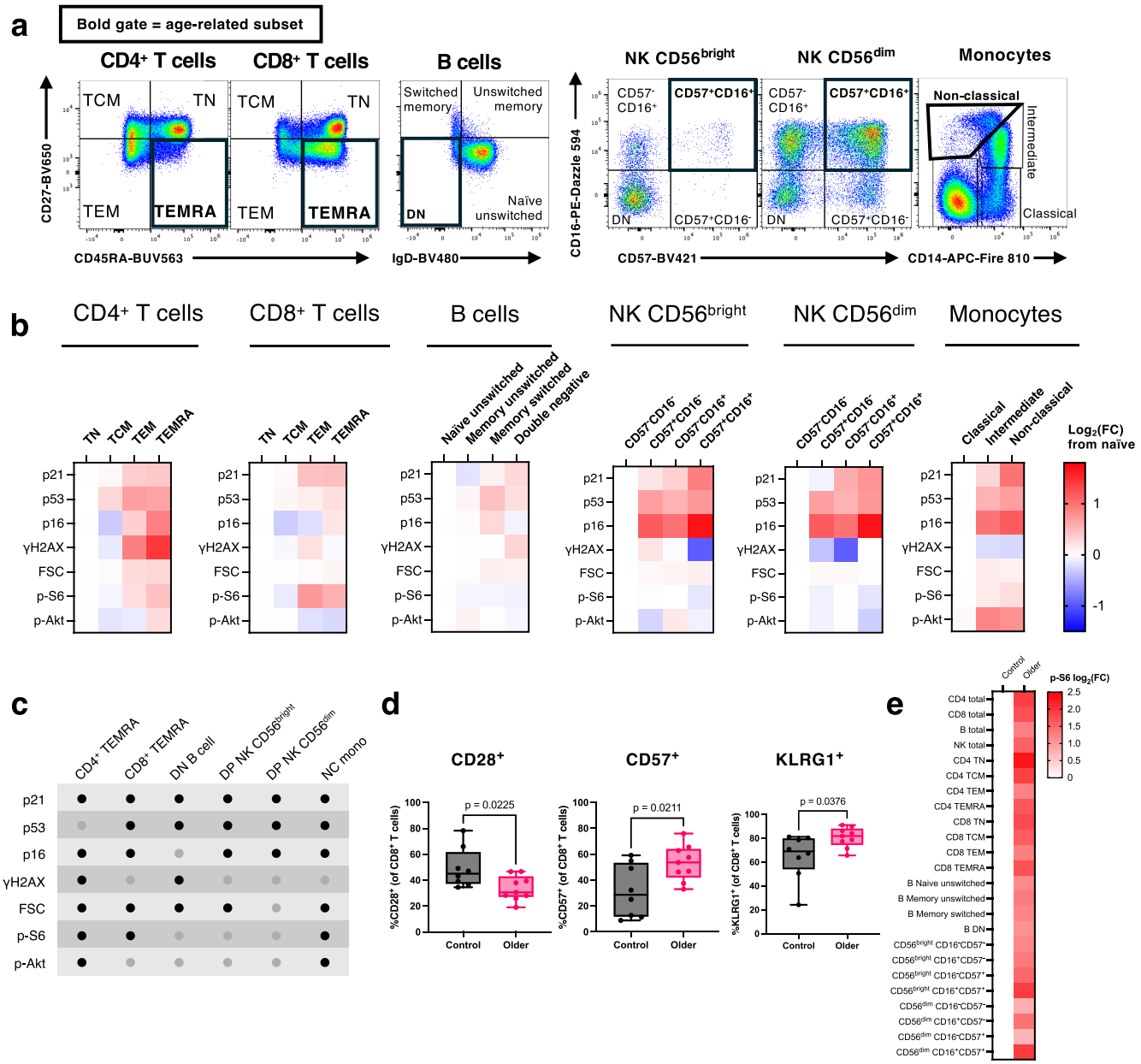

FIGURE 5 | Age-related peripheral immune subsets from healthy donors display elevated markers of cellular senescence and mTORC1/2 hyperactivity. (a) Immune cell subsets in PBMCs from a healthy donor identified by flow cytometry. Gates highlighted in bold indicate age-related immune subsets. (b) Geometric mean fluorescence intensity (gMFI) of biomarkers for senescence and mTORC1/2 activity as measured by spectral flow cytometry across immune subsets in $n = 8$ healthy donors. Data represent $\log_2$(fold change) from the mean of the left-hand, most early-differentiated immune cell population for each cell type. FSC = forward scatter. (c) Table summarising significantly increased markers (black dots) in age-related immune subsets compared to early-differentiated immune cell counterparts, as assessed with one-way ANOVAs with Dunnett's multiple comparisons test between age-related and early-differentiated subsets for each cell type ($n = 8$ healthy donors). (d) Proportion of $CD8^+$ T cells positive for CD28, CD57 and KLRG1 in PBMCs from healthy younger donors (17–50 years old, $n = 8$) and older donors (56–69 years old, $n = 9$). p-values are derived from unpaired t-tests. (e) Geometric mean fluorescence intensity (gMFI) of p-S6 in immune subsets in older donors ($n = 9$) expressed as $\log_2$ (fold change) from the mean value of cells of control donors ($n = 8$), assessed by flow cytometry.

γH2AX-marked DNA damage, 4-month rapamycin treatment caused a robust and significant decrease in p21 expression across most immune cell subsets studied, reflecting the attenuation of DNA damage-induced p21 with rapamycin we observed in vitro (Figure 6e). p53 expression was elevated at 4 months in PBMCs from the rapamycin-treated compared to the placebo groups (Figure 6f). A previous study demonstrated that in vivo mTOR inhibition decreased the percentage of circulating PD-1^+ T cells (Mannick et al. 2014). Though we did not observe changes in PD-1 in the current study (Figure S7d), the proportion of T cells expressing other immune co-inhibitory molecules, such as KLRG1 (Figure 6g), NKG2A (Figure 6h) and LAG3 (Figure 6i), was reduced in the T cells from rapamycin compared to placebo groups. Overall, these results suggest that rapamycin reduces the expression of immune exhaustion markers, and p21, a marker of both persistent DNA damage and cell senescence.

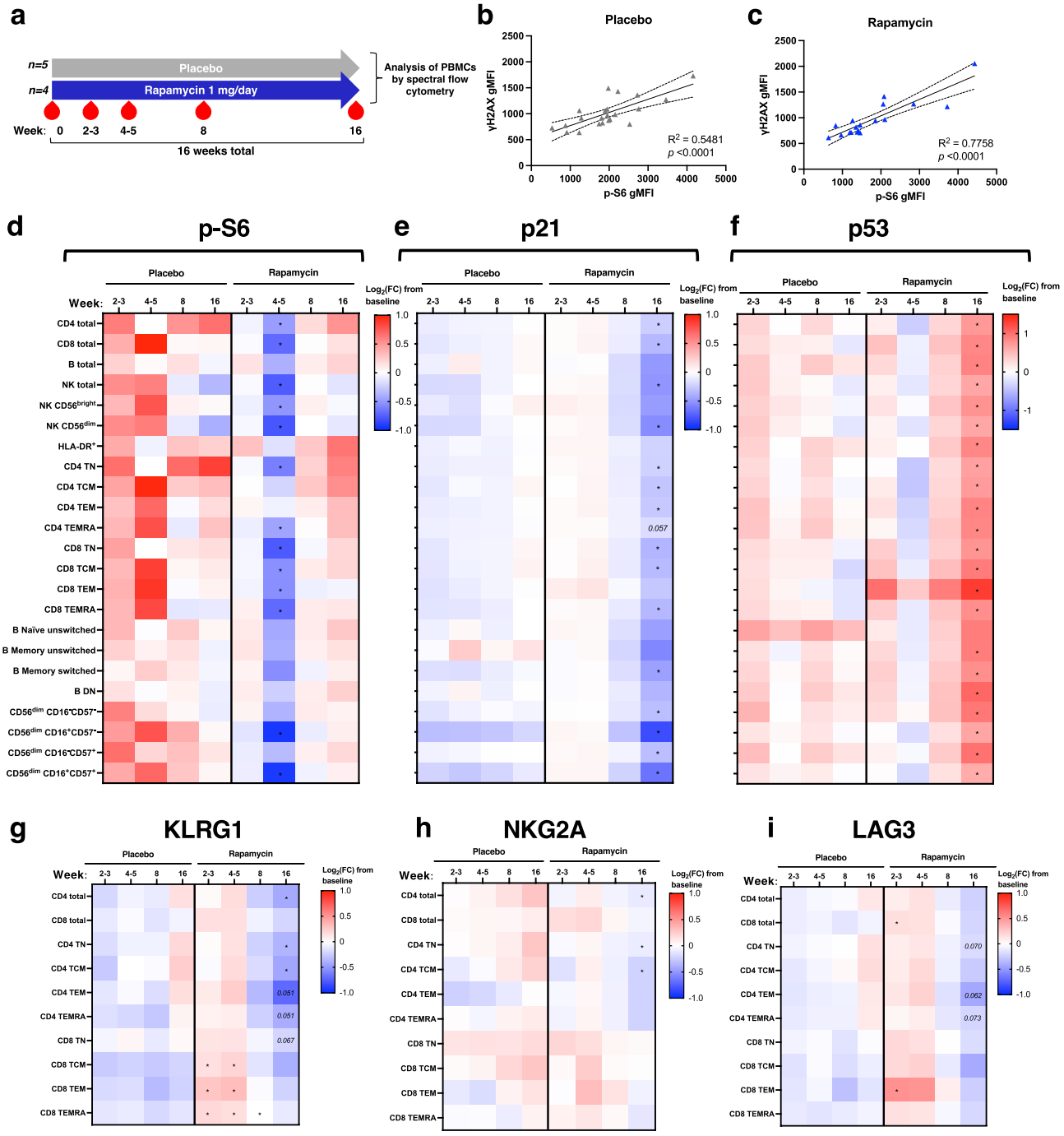

FIGURE 6 | Low-dose rapamycin in vivo attenuates biomarkers of immune cell senescence and exhaustion. (a) Outline of the in vivo rapamycin study. (b, c) Simple linear regression analyses of γH2AX and p-S6 geometric fluorescence intensity (gMFI) over all timepoints in $CD4^+$ T cells from (b) placebo and (c) rapamycin groups. Graphs show line of best-fit with 95% confidence intervals. (d–f) Log_2(fold change) from baseline in gMFI of (d) p-S6, (e) p21 and (f) p53 across immune subsets. (g-i) Percentage of defined T cell subsets positive for (g) KLRG1, (h) NKG2A and (i) LAG3 in participants. In (d, e), each value is expressed as log_2(fold change) from baseline for each participant. *p*-values are derived from an unpaired *t*-test between placebo ($n = 5$) and rapamycin ($n = 4$) at each time point. Statistically significant ($p < 0.05$) *p*-values are indicated.

TABLE 2 | Baseline characteristics of participants in the in vivo rapamycin study.

	Placebo ($n = 5$)	Rapamycin ($n = 4$)	*p*-value
Age (years)	64.2 ± 5.34	60.0 ± 4.62	0.1667 (ns)
BMI (kg/m^2)	26.4 ± 3.31	27.1 ± 1.24	> 0.9999 (ns)

Note: Data are presented as mean ± SD. *p*-values are derived from Mann–Whitney tests.
Abbreviation: ns = not significant.

While participant numbers in the rapamycin in vivo study are low, the changes in DNA damage and senescence markers are significant.

3 | Discussion

While mTOR inhibition is a well-known and potent anti-ageing intervention in animal models, an explanation for its ability to extend health- and lifespan so reproducibly has been lacking (Weichhart 2018; Sharp and Strong 2023). Furthermore, our understanding around why mTOR inhibitors have shown benefit in boosting immune resilience in older people is incomplete. In this study, we have demonstrated for the first time that mTOR inhibitors can protect T cells from DNA damage and senescence marker upregulation after exposure to a genotoxic agent. We show that this is through a mechanism independent of autophagy, cell cycle progression, and protein synthesis. Rather, we show that this is through a mitigation of DNA lesional burden, affording a greater survival following exposure to DNA-damaging treatment. This enhancement of protection from DNA damage, which we call genoprotection, offers a new explanation for previous studies that have demonstrated an attenuation of replicative senescence with mTOR inhibitors in 2D cell culture (Walters et al. 2016; Park et al. 2020; Iglesias-Bartolome et al. 2012) and in vivo in human skin (Chung et al. 2019), and its potent geroprotective ability. Our study also provides a novel explanation for previous reports which show that rapamycin improves aged antigen-specific immunity in mouse models of immunosenescence bearing immune-specific knockout of DNA repair (Yousefzadeh, Flores, et al. 2021). Furthermore, our findings expand on previous research showing a reduction in DNA damage markers with rapamycin in irradiated normal oral keratinocytes (Iglesias-Bartolome et al. 2012), DNA repair-deficient fibroblasts (Saha et al. 2014), human oocytes undergoing in vitro maturation (Yang et al. 2022), DNA repair-deficient mouse podocytes (Braun et al. 2025), and lymphocytes of kidney transplant patients (Chebel et al. 2016). In the cited studies, enhanced resilience to DNA damage with mTOR inhibition was shown to arise from several sources, including heightened expression of antioxidant enzymes, such as mitochondrial superoxide dismutase, that limit ROS and genotoxic stress (Iglesias-Bartolome et al. 2012), and increased protein expression of the DNA repair factors, MGMT and NDRG1, via a post-transcriptional mechanism (Dominick et al. 2017). Our data from human immune cells may therefore reflect a universal impact of rapamycin on promoting genome integrity in eukaryotes.

In the present study, we asked whether age-related immune cells from diverse haematopoietic lineages exhibited DNA damage-induced senescence, by comprehensively profiling senescence markers in human immune subsets using high-dimensional spectral cytometry. Our data are the first to show that age-related immune subsets from diverse immune lineages, in $CD4^+$ and $CD8^+$ T cells, B cells, NK cells, and monocytes, are uniformly enriched for senescence biomarkers. In particular, the DNA damage-induced cyclin kinase inhibitor, p21, was a senescence marker upregulated in most age-related immune subsets. This suggests that the form of senescence which immune cells undergo with ageing may be p53- and p21-driven, hinting—importantly—towards a more DNA damage-induced type of senescence, consistent with other evidence that DNA damage plays a central role in the decline of immune system function (Kell et al. 2023). We note that senescence in immune cells may manifest differently from senescence in other cell types, such as fibroblasts, predominantly by their ability to maintain some, albeit poor, proliferative capacity (Akbar et al. 2016). Like age-related immune subsets, immune cells from older donors exhibited higher levels of p-S6, indicating mTORC1 activity, suggesting that, like ageing of other human tissues (Markofski et al. 2015), immune ageing is associated with mTORC1 hyperactivity.

Most importantly, our findings translate to the in vivo condition in humans. Through a small pilot study with limited participant numbers, our data are the first to demonstrate a significant reduction in p21-marked cellular senescence upon 4-month, low-dose rapamycin treatment vs placebo in immune cells in the blood of older people. We also found that rapamycin increased p53 levels in circulating immune cells. p53 serves multiple physiological roles in vivo; for example, in addition to its well-known role in signal transduction of acute DNA damage, it also regulates mitochondrial respiration—indeed, mice null for p53 have very poor exercise tolerance with early fatigue onset (Bartlett et al. 2014). Though at this stage highly speculative, it is possible that elevated p53 in immune cells from rapamycin-treated participants may indicate better overall metabolic health. In addition, enhancement of p53 expression has been shown recently to improve DNA repair after irradiation-induced senescence of human dermal fibroblasts (Miller et al. 2025). Therefore, while p53 was suppressed by rapamycin following acute DNA damage in vitro, our observation that longer-term rapamycin administration in older individuals increases p53 levels may reflect improved genome integrity.

A recent study from our group showed that poor COVID vaccine memory responses in older people (vaccine non-responders) were linked to higher levels of immune cell senescence, characterised by high mTOR activity, p16 expression and γH2AX-marked DNA damage (Alsaleh et al. 2024). mTOR hyperactivity and immune cell senescence in older people, which we have also observed in our study, may therefore be functionally related to impaired antigen-specific responses. Spermidine supplementation improved adaptive immune responses post-vaccination and correspondingly led to decreased p16 expression and mTOR activity in aged immune cells, particularly in vaccine non-responders (Alsaleh et al. 2024). Unlike spermidine, rapamycin decreased immune cell p21 expression in our study, suggesting that these two interventions impact distinct pathways to reverse immune cell senescence in older people, which should be further investigated.

Similar to the clinical trial administering spermidine (Alsaleh et al. 2024), our findings using rapamycin allow us to speculate that the positive effect of 6-week treatment with the rapalogue RAD001 (everolimus) on boosting flu vaccine responses and respiratory infections may be through an attenuation of immune cell DNA damage and subsequent senescence (Mannick et al. 2018; Mannick et al. 2014). In the cited studies by Mannick et al., everolimus caused a reduction in the proportion of circulating $PD\text{-}1^+$ $CD4^+$ and $CD8^+$ T cells (Mannick et al. 2014). In our study, we observed a significant reduction in both $KLRG1^+$ and $NKG2A^+$ $CD4^+$ T cells and near-significantly $LAG3^+$ $CD4^+$

T cells in the rapamycin compared to placebo groups. Like PD-1, these three cell-surface proteins are all immune checkpoint inhibitors, each with roles in limiting T cell activation. Therefore, we observed similar functional effects of rapamycin as perhaps potentiating a less-exhausted T cell phenotype. Overall, based on our in vitro effects mTOR inhibitors and in vivo effects of rapamycin, we suggest that rapamycin positively enhances genome stability and therefore targets a central hallmark of ageing (Lopez-Otin et al. 2023).

Our discovery that mTOR inhibitors are genoprotective makes them amenable for use in a wide range of clinical scenarios where the induction of DNA damage leads to pathology. For example, cancer treatments such as radio- or chemotherapy lead to widespread DNA damage of healthy tissue; thus, treatment with a genoprotector, such as low-dose rapamycin, after remission from the original tumour may attenuate the accelerated ageing associated with such cancer therapies (Wang et al. 2024). Likewise, exposure to the space environment, and especially the DNA instability caused by cosmic radiation, is of increasing concern as space travel becomes more commonplace (Beheshti et al. 2021). Our study, through its novel identification of rapamycin as a genoprotector, suggests potential avenues for mitigating these harmful DNA-damaging effects of space travel.

Genoprotectors such as rapamycin present a new and exciting therapeutic approach for the treatment of age-related diseases, both infectious and chronic in nature. SARS-CoV-2, the virus behind the COVID-19 pandemic, induces DNA damage and senescence by degrading DDR enzymes (Gioia et al. 2023); heightened virus-induced senescence in this way strongly contributes to disease mortality (Camell et al. 2021; Lee et al. 2021). Perhaps prophylactic treatment of older care home residents with genoprotectors such as low-dose mTOR inhibitors may provide a much-needed boost to genome stability and immune resilience in this vulnerable population during future pandemics (Cox et al. 2020). Likewise, since mTOR inhibitors improve vaccine responses in older people (Mannick et al. 2018; Mannick et al. 2021; Mannick et al. 2014), future vaccine drives could consider administering short-term mTOR inhibition treatments prior to immunisations against pathogens that particularly affect the older population, such as influenza, coronaviruses and VZV. Infections by other pathogens, such as *Salmonella Typhi*, *Leishmania* and some Gram-negative bacteria (which release cytolethal distending toxin), all drive pathology through the induction of DNA damage and senescence (Ibler et al. 2019; Mathiasen et al. 2021; Covre et al. 2018); low-dose mTOR inhibition in these contexts of infection could possibly limit genome instability and disease progression. Though largely untested in humans, research in mice at least suggests that rapamycin improves immune control of Leishmaniasis (Khadir et al. 2018). Finally, in addition to progeroid diseases resulting from a DNA repair deficiency (Werner syndrome, Rothmund-Thomson syndrome, Bloom syndrome, Cockayne's syndrome, Fanconi's anaemia and Ataxia-Telangiectasia), chronic viral infection and rheumatic diseases exhibit decreased DNA repair factor expression in immune cells (Zhao et al. 2018; Shao et al. 2009; Li et al. 2016). It is possible, though unexplored, that rapamycin could limit DNA damage and attenuate pathology in these diseases.

Given the known physiological roles of senescent cells and DNA damage, caution must be taken in administering genoprotective low-dose mTOR inhibitors (de Magalhaes 2024). For example, inhibiting seno-conversion of virus-infected cells may disrupt their removal by the immune system. Additionally, genoprotectors may disrupt the intentional induction of DNA damage by adaptive immune cells during VDJ recombination, potentially leading to immunodeficiency; however, as the thymus (where T cell VDJ recombination occurs) atrophies with age, it is likely that late-life administration of low-dose rapamycin would not impact T cell development, but possibly B cell maturation. Finally, senescent cells play critical roles in tissue regeneration in response to damage (Chen et al. 2023); thus, genoprotectors may have unforeseen consequences such as hindering wound healing, a process which is already impaired in older people (Demaria et al. 2014; Wicke et al. 2009).

Taken together, our findings of immune cell benefit on rapamycin treatment in vitro and from analysis of PBMCs from an in vivo study using low-dose rapamycin lead us to conclude that rapamycin at 1 mg/day enhances the resilience of the ageing immune system to DNA damage. Our findings support the initiation of phase 2 double-blind placebo-controlled studies of rapamycin to support healthy immunity and reduce immunosenescence in at-risk older adults.

4 | Materials and Methods

4.1 | Ethical Approval for Study

Healthy control blood was taken with fully informed consent under ethical approval from the Local Research Ethics Committee (REC) at the University of Oxford, reference 11/H0711/7, to cover the use of human blood products purchased from National Health Services Blood and Transplant service (NHS England). PBMCs from participants undergoing 4-month rapamycin or placebo treatment were obtained under ethical approval by the Local REC at the University of Nottingham Faculty of Medicine and Health Sciences, reference FMHS 90-0820. We registered this study on ClinicalTrials.gov (ID: NCT05414292) although it was not necessary to do so, as our study was designated as a 'human physiology' and not a clinical trial. Healthy older male participants (aged between 50 and 90 years old) were randomised into two groups and received either 1 mg/day rapamycin (Pfizer, Belgium) or a placebo sucrose/lactose tablet (Hsconline) for 4 months. All participants gave informed consent to participate in the study. Participants included had a BMI between 18 and 35 kg/m^2, and no active cardiovascular, cerebrovascular, respiratory or metabolic disease, clotting dysfunction, no history of neurological or musculoskeletal conditions, had not taken part in a recent study in the last 3 months, and did not have contraindications either to MRI scanning or rapamycin. PBMCs were isolated at 5 time points over 4 months of intervention (rapamycin and placebo) using Ficoll-Paque gradient centrifugation as described below. After 8 weeks of treatment, white blood cell counts were quantified in the Royal Derby Hospital Pathology laboratory using a Sysmex XN-Series analyser, and blood rapamycin concentration measured using LC–MS (described below).

4.2 | Measurement of Blood Rapamycin Concentration Using LC–MS

50 μL of D3-labelled rapamycin was added to 50 μL of whole blood, before adding 100 μL of precipitation reagent (70: 30, Methanol:0.3 M Zinc Sulfate). Samples were vortexed for 30 s and mixed on a Vibrax shaker at RT (1000 rpm) for 10 min. Samples were then centrifuged at 10000*g* for 10 min at 4°C. Supernatant was aliquoted into a 2 mL screw top autosampler vial with low volume insert, before injection into the LC–MS. Samples were quantified against a standard curve of known rapamycin concentrations ranging from 50 ng/mL to 0.39 ng/mL prepared in the same way as the samples. Analysis was performed using a Waters ACQUITY UHPLC attached to a Thermo Scientific TSQ Quantum Ultra MS. Rapamycin was isolated using an Agilent Zorbax SB-Aq Narrow Bore RR Column (2.1 mm × 100 mm × 3.5 μm) and a binary buffer system of 2 mM Ammonium Acetate in Water (Buffer A) and 2 mM Ammonium Acetate in Methanol (Buffer B) at a flow rate of 0.3 mL/min. Gradient conditions were as follows: 80% B for 0.5 min, 80% B to 90% B 0.5–2 min, 99% B 2–6 min, 99% B to 80% B 6–6.5 min, 80% B 6.5–10 min. Rapamycin was detected using single reaction monitoring (SRM) for m/z transitions of 931.6 m/z—864.66 m/z for unlabelled rapamycin and 934.520–864.660 for D3-labelled rapamycin.

4.3 | PBMC Isolation and Culture

Fresh blood was either collected in EDTA tubes (9 mL) or in blood cones (10 mL) as concentrated by-products of the apheresis process, supplied by the National Health Service Blood and Transplant service (NHS England). PBMCs were isolated using standard Ficoll density gradient centrifugation. Briefly, blood was diluted 1:1 in sterile Dulbecco's PBS (DPBS, 1:5 for blood cones) (Sigma-Aldrich) and 15 mL gently pipetted over 20 mL Histopaque-1077 (Sigma) before centrifugation at 500 g for 30 min at room temperature with minimum deceleration. The PBMC layer was collected by aspiration and washed twice in DPBS. PBMC number was determined by mixing 1:1 (v/v) with Trypan Blue (Sigma) and counting using a haemocytometer. For cryopreservation, PBMCs were resuspended at 5×10^6 cells/ml in freezing medium (50% FBS, 40% RPMI 1640, 10% DMSO [all Sigma]) and placed at −80°C before transferral to a liquid nitrogen facility (−196°C) for long-term storage. Peripheral blood mononuclear cells (PBMCs) were cultured in R10 (RPMI 1640 (Gibco) containing penicillin (100 U/mL) and streptomycin (100 μg/mL) (both Sigma) and 10% FBS), in a humidified incubator with 5% CO_2 at 37°C. Details of the drugs used for in vitro assays are provided in Table S1.

4.4 | DNA Damage Assay in PBMCs

Cryopreserved PBMCs were thawed in R10 (10 mL per 1 cryovial of cells) and centrifuged at 500*g* for 5 min. The supernatant was removed, and cells resuspended in R10 at a concentration of 1×10^6 cells/ml and allowed to recover overnight in R10. The next day, PBMCs were subjected to T cell-specific activation using antibodies targeting CD3 (clone OKT3) and CD28 (clone CD28.2) at 1 μg/mL final concentration (both BioLegend) in the presence of drug treatment or vehicle, where appropriate, for 3 days. Where specified for individual experiments, $CD4^+$ T cells were isolated by negative selection on a magnetic column using a kit (Miltenyi) and subsequently activated in wells of a 24-well plate (pre-coated with 1 μg/mL anti-CD3 in PBS for 2 h at 37°C) with 1 μg/mL anti-CD28 in the culture media, for 3 days ($0.5–1 \times 10^6$ cells/mL). After 3 days, cells were harvested by trituration, centrifuged at 500*g* for 5 min and resuspended and incubated in R10 with 200 μg/mL zeocin for 2 h or 25 μM H_2O_2 for 15 min (Table S1), in a 24-well plate. As both zeocin and H_2O_2 are soluble directly in water and cell culture medium, negative controls were not treated with solvent. Cells were then washed in R10 and allowed to recover for a defined period (see individual figures) before being collected for further downstream analysis. Where specified, the DNA damage assay was performed in the presence of rapamycin (10 nM), AZD8055 (100 nM) or chloroquine (10 μM) (drug details provided in Table S1).

4.5 | Staining for Conventional Flow Cytometry

Cells were pelleted at 500 g for 5 min and resuspended in 50 μL of a master mix of cell-surface-staining antibodies diluted in FACS buffer (0.2% BSA (w/v), 2 mM EDTA in PBS) and Zombie NIR Live/Dead viability dye (1/1000 dilution, BioLegend) with incubation for 30 min at 4°C. Cells were washed in FACS buffer and fixed for 20 min at 4°C in BD Cytofix Fixation Buffer (BD Biosciences). Permeabilisation of cells was performed by washing cells in 1X BD Phosflow Perm/Wash Buffer I (BD Biosciences), followed by incubation in the permeabilisation buffer for 10 min at RT in the dark. Intracellular antibody staining was performed overnight at 4°C in the dark in BD Phosflow Perm/Wash Buffer I. When necessary, staining of unconjugated primary antibodies with a fluorescence-conjugated secondary antibody was performed in BD Phosflow Perm/Wash Buffer I for 1 h at RT in the dark. Cells were washed once more and stored in FACS buffer prior to acquisition on a flow cytometer (BD LSRFortessa) and analysis using FlowJo version 10.9.0 (gating strategy in Figure S1). Compensation analysis was performed using single-stained compensation beads (Thermo Fisher or BioLegend). Details of antibodies used for flow cytometry staining are provided in Table S2.

4.6 | Staining for Spectral Flow Cytometry

PBMCs were stained for analysis for spectral flow cytometry as above, with some modifications. First, cells were harvested and pelleted (500 g for 5 min) and incubated in 50 μL solution containing LIVE/DEAD Fixable Blue Dead Cell Stain Kit (1/400 dilution, Invitrogen) and FcR blocking reagent (1/400 dilution, Miltenyi) in PBS for 15 min at 4°C. Surface and intracellular antigen staining was then performed as above. After staining, cells were filtered through a 70 μm Flowmi cell strainer (Sigma) to remove aggregates before analysis on a 5-laser (R/B/V/YG/UV) Aurora spectral flow cytometer (Cytek Biosciences). For each experiment, all samples were processed in one batch and single-colour cell- and bead-based controls were generated in parallel alongside the sample staining for spectral unmixing. Details of antibodies used for spectral flow

cytometry staining are provided in Table S2. The gating strategy is provided in Figure S6.

4.7 | Autophagic Flux Analysis

Measurement of autophagic flux in cells was performed using an antibody-based LC3 assay kit (Cytek Biosciences) with the following modifications (Figure S3). 2 h prior to LC3 staining, each sample of cells was divided for treatment either with 10 nM Bafilomycin A_1 (Table S1) or vehicle (0.1% DMSO final concentration) in R10. Cells were harvested and incubated in Live/Dead viability dye (1/1000 dilution, BioLegend) and FcR blocking reagent (1/400 dilution, Miltenyi) in PBS for 15 min at 4°C, then surface staining with antibodies was performed as described above, followed by washing in 1X assay buffer (Cytek Biosciences) diluted in dH_2O, and subsequently permeabilised using 0.05% saponin (w/v) (Thermo Scientific) in PBS for 3 min at RT. Cells were then incubated with an LC3-FITC conjugated antibody (Table S2) in 1X assay buffer for 30 min at 4°C. For co-staining of LC3 with an anti-γH2AX antibody (Table S2), the incubation time was increased to 1 h in 1X assay buffer. After staining, cells were then washed in 1X assay buffer and fixed in 2% PFA for 10 min at RT, before being finally resuspended in FACS buffer and acquired on an LSRFortessa cytometer (BD) or 5-laser Aurora spectral flow cytometer (Cytek) (Figure S3) and analysed using FlowJo version 10.9.0. Autophagic flux was calculated from the mean fluorescence intensity (MFI) of LC3 in Bafilomycin A_1- and vehicle-treated conditions ($LC3_{BafA}$ and $LC3_{Veh}$, respectively) using the formula:

$$\text{Autophagic flux} = \frac{\text{LC3}_{\text{BafA}} - \text{LC3}_{\text{Veh}}}{\text{LC3}_{\text{Veh}}}$$

4.8 | Cell Cycle Phase Distribution Analysis

To assess cell cycle phase distribution using flow cytometry, cells were incubated for 4 h with 10 μM of 5-ethynyl-2′-deoxyuridine (EdU) (Invitrogen). Cells were then harvested and incubated in Live/Dead viability dye (1/1000 dilution, BioLegend) and FcR blocking reagent (1/400 dilution, Miltenyi) in PBS for 15 min at 4°C. After this, surface antigen staining for flow cytometry was performed as described above. DNA-incorporated EdU was identified via a click chemistry reaction according to the manufacturer's instructions (Invitrogen), followed by overnight staining for intracellular γH2AX as described above. Cells were then washed and incubated with FxCycle Violet Stain for DNA (1/1000 dilution, Invitrogen) in permeabilisation buffer (from EdU kit, Invitrogen) and analysed on an LSR Fortessa X-20 cytometer (BD) and FlowJo version 10.9.0.

4.9 | Protein Synthesis Assay

Nascent protein synthesis was measured using the Click-iT Plus OPP Alexa Fluor 594 Protein Synthesis Assay Kit (Invitrogen). Cells were incubated with 20 μM O-propargyl-puromycin (OPP, from the kit) for 30 min, then collected and stained for surface antigens. Cells treated for 1 h with 50 μg/mL cycloheximide (Table S1) served as a positive control for protein synthesis inhibition. Cells were subsequently fixed, permeabilised and polypeptide-incorporated OPP was detected, according to the manufacturer's instructions. Cells were analysed on a Fortessa X-20 flow cytometer (BD) and FlowJo version 10.9.0.

4.10 | Alkaline Comet Assay

SuperFrost Plus Adhesion slides (VWR) were first pre-coated with normal melting point agarose (NMPA) (1% (w/v) in dH_2O, Sigma) and allowed to dry overnight. Following treatments, cells were harvested by trituration and resuspended in PBS at a concentration of 2×10^5 cells/ml. 250 μL of the cell suspension was mixed with 1 mL of low melting point agarose (1% w/v in PBS, Sigma) pre-warmed to 37°C, and 1 mL of the mixture was pipetted onto one NMPA-coated slide. Coverslips were then placed on the slides and left to gel on ice. For the lysis of cells, coverslips were removed, and slides were incubated overnight at 4°C in fresh, ice-cold lysis buffer (2.5 M NaCl, 100 mM EDTA, 10 mM Tris base containing 1% DMSO (v/v) and 1% Triton X-100 (v/v), pH 10.5). The next day, slides were incubated for 30 min in the dark with fresh alkaline electrophoresis buffer (300 mM NaOH, 1 mM EDTA and 1% DMSO (v/v), pH > 13). Slides were then electrophoresed in the dark for 25 min at 1 V/cm (distance between electrodes), at a constant current of 300 mA. Slides were then neutralised with 3 × 5 min incubations in neutralisation buffer (500 mM Tris–HCl, pH 8.1) and subsequently left to dry overnight. The next day, slides were rehydrated for 30 min in dH_2O, and DNA was stained for 30 min with 1X SYBR Gold Nucleic Acid Gel Stain (Invitrogen) in dH_2O. Comets were visualised with a Zeiss Axio Imager and analysed using the OpenComet plugin in Fiji version 2.3.0.

4.11 | Statistical Tests and Figures

All statistical and (log)normality testing of data was performed using GraphPad Prism version 10.0.0. *p*-values indicating statistical significance are either indicated exactly or represented as: ns (not significant) $p > 0.05$, *$p \leq 0.05$, **$p \leq 0.01$, ***$p \leq 0.001$, ****$p \leq 0.0001$. Unless otherwise stated, bar graph data always represent mean ± SEM. Box-and-whisker plots always show minimum to maximum values, with the median, 25th, and 75th percentiles indicated. Figures were made using Microsoft PowerPoint version 16.88. Graphical abstract was created with BioRender.com.

Author Contributions

Loren Kell, **Lynne S. Cox**, **Anna K. Simon**, **Ghada Alsaleh**, **Philip J. Atherton**, **Kenneth Smith:** conceptualization. **Loren Kell**, **Eleanor J. Jones**, **Daniel J. Wilkinson**, **Nima Gharahdaghi**, **Ghada Alsaleh:** methodology. **Loren Kell**, **Eleanor J. Jones**, **Daniel J. Wilkinson**, **Nima Gharahdaghi:** investigation. **Loren Kell:** visualisation. **Lynne S. Cox**, **Anna K. Simon**, **Ghada Alsaleh**, **Philip J. Atherton:** funding acquisition. **Lynne S. Cox**, **Anna K. Simon**, **Ghada Alsaleh**, **Philip J. Atherton**, **Eleanor J. Jones**, **Loren Kell**, **Daniel J. Wilkinson**, **Kenneth Smith:** project administration.

Ghada Alsaleh, **Lynne S. Cox**, **Anna K. Simon:** supervision. **Loren Kell:** writing – original draft. **Loren Kell**, **Lynne S. Cox**, **Ghada Alsaleh**, **Anna K. Simon:** writing – review and editing.

Funding

This work was supported by the following grants: the Mellon Longevity Graduate Programme at Oriel College, University of Oxford (Loren Kell, Lynne S. Cox); UK SPINE (Research England) proof-of-concept grant (Lynne S. Cox, Philip J. Atherton, Daniel J. Wilkinson, Anna K. Simon); Wellcome Trust (Anna K. Simon); Helmholtz Association (Anna K. Simon); Versus Arthritis grant 22617 (Ghada Alsaleh); BBSRC (the Biotechnology and Biological Sciences Research Council) grant BB/W01825X/1 (Lynne S. Cox); MRC (Medical Research Council) (Lynne S. Cox); MRC grant MR/P021220/1 as part of the MRC-Versus Arthritis Centre for Musculoskeletal Ageing Research awarded to the Universities of Nottingham and Birmingham (Philip J Atherton, Daniel J. Wilkinson); Public Health England (now UK Health Security Agency) (Lynne S. Cox); Diabetes UK/BIRAX (Lynne S. Cox).

Conflicts of Interest

Anna K. Simon consults for Oxford Healthspan, The Longevity Labs and Calico. Lynne S. Cox is Program Director of Wellcome Leap's Dynamic Resilience program (co-funded by Temasek Trust), and has recently served as co-director of UKRI-funded UK Ageing Research Networks (UKAN) and the BLAST ageing research network (UKRI funded), and co-chair of the European Geriatric Medicine Society special interest group in Ageing Biology. Ghada Alsaleh, Eleanor J. Jones, Nima Gharahdaghi, Daniel J. Wilkinson, Philip J. Atherton, Kenneth Smith and Loren Kell report no conflicts of interest.

Data Availability Statement

All data are available in the main text or the Supporting Information.

References

Akbar, A. N., S. M. Henson, and A. Lanna. 2016. "Senescence of T Lymphocytes: Implications for Enhancing Human Immunity." *Trends in Immunology* 37: 866–876.

Alsaleh, G., M. Ali, A. Kayvanjoo, et al. 2024. "Spermidine Mitigates Immune Cell Senescence, Enhances Autophagy, and Boosts Vaccine Responses in Healthy Older Adults."

Alsaleh, G., I. Panse, L. Swadling, et al. 2020. "Autophagy in T Cells From Aged Donors Is Maintained by Spermidine and Correlates With Function and Vaccine Responses." *eLife* 9: e57950.

Altomare, J. F., R. E. Smith, S. Potdar, and S. H. Mitchell. 2006. "Delayed Gastric Ulcer Healing Associated With Sirolimus." *Transplantation* 82: 437–438.

Bartlett, J. D., G. L. Close, B. Drust, and J. P. Morton. 2014. "The Emerging Role of p53 in Exercise Metabolism." *Sports Medicine* 44: 303–309.

Beheshti, A., J. T. Mcdonald, M. Hada, A. Takahashi, C. E. Mason, and M. Mognato. 2021. "Genomic Changes Driven by Radiation-Induced DNA Damage and Microgravity in Human Cells." *International Journal of Molecular Sciences* 22: 10507.

Bjedov, I., J. M. Toivonen, F. Kerr, et al. 2010. "Mechanisms of Life Span Extension by Rapamycin in the Fruit Fly Drosophila Melanogaster." *Cell Metabolism* 11: 35–46.

Bonassi, S., M. Ceppi, P. Moller, et al. 2021. "DNA Damage in Circulating Leukocytes Measured With the Comet Assay May Predict the Risk of Death." *Scientific Reports* 11: 16793.

Braun, F., A. M. Mandel, L. Blomberg, et al. 2025. "Loss of Genome Maintenance Is Linked to mTOR Complex 1 Signaling and Accelerates Podocyte Damage." *JCI Insight* 10: e172370.

Callender, L. A., E. C. Carroll, E. A. Bober, A. N. Akbar, E. Solito, and S. M. Henson. 2020. "Mitochondrial Mass Governs the Extent of Human T Cell Senescence." *Aging Cell* 19: e13067.

Camell, C. D., M. J. Yousefzadeh, Y. Zhu, et al. 2021. "Senolytics Reduce Coronavirus-Related Mortality in Old Mice." *Science* 373: eabe4832.

Carroll, B., G. Nelson, Y. Rabanal-Ruiz, et al. 2017. "Persistent mTORC1 Signaling in Cell Senescence Results From Defects in Amino Acid and Growth Factor Sensing." *Journal of Cell Biology* 216: 1949–1957.

Chebel, A., R. Catallo, C. Mabon, et al. 2016. "Rapamycin Safeguards Lymphocytes From DNA Damage Accumulation In Vivo." *European Journal of Cell Biology* 95: 331–341.

Chen, C., Y. Liu, Y. Liu, and P. Zheng. 2009. "mTOR Regulation and Therapeutic Rejuvenation of Aging Hematopoietic Stem Cells." *Science Signaling* 2: ra75.

Chen, C., M. Saclier, J. Chantrel, S. Mella, A. Chiche, and H. Li. 2023. "Single-Cell RNAseq Reveals the Pro-Regenerative Role of Senescent FAPs in Muscle Regeneration." *bioRxiv*. https://doi.org/10.1101/2023.12.12.571148.

Chung, C. L., I. Lawrence, M. Hoffman, et al. 2019. "Topical Rapamycin Reduces Markers of Senescence and Aging in Human Skin: An Exploratory, Prospective, Randomized Trial." *Geroscience* 41: 861–869.

Colonna-Romano, G., M. Bulati, A. Aquino, et al. 2009. "A Double-Negative (IgD-CD27-) B Cell Population Is Increased in the Peripheral Blood of Elderly People." *Mechanisms of Ageing and Development* 130: 681–690.

Covre, L. P., R. F. Martins, O. P. Devine, et al. 2018. "Circulating Senescent T Cells Are Linked to Systemic Inflammation and Lesion Size During Human Cutaneous Leishmaniasis." *Frontiers in Immunology* 9: 3001.

Cox, L. S., I. Bellantuono, J. M. Lord, et al. 2020. "Tackling Immunosenescence to Improve COVID-19 Outcomes and Vaccine Response in Older Adults." *Lancet Healthy Longevity* 1: e55–e57.

Czesnikiewicz-Guzik, M., W. W. Lee, D. Cui, et al. 2008. "T Cell Subset-Specific Susceptibility to Aging." *Clinical Immunology* 127: 107–118.

de Magalhaes, J. P. 2024. "Cellular Senescence in Normal Physiology." *Science* 384: 1300–1301.

Demaria, M., N. Ohtani, S. A. Youssef, et al. 2014. "An Essential Role for Senescent Cells in Optimal Wound Healing Through Secretion of PDGF-AA." *Developmental Cell* 31: 722–733.

Desdin-Mico, G., G. Soto-Heredero, J. F. Aranda, et al. 2020. "T Cells With Dysfunctional Mitochondria Induce Multimorbidity and Premature Senescence." *Science* 368: 1371–1376.

Dominick, G., J. Bowman, X. Li, R. A. Miller, and G. G. Garcia. 2017. "mTOR Regulates the Expression of DNA Damage Response Enzymes in Long-Lived Snell Dwarf, GHRKO, and PAPPA-KO Mice." *Aging Cell* 16: 52–60.

Frasca, D., A. Diaz, M. Romero, and B. B. Blomberg. 2017. "Human Peripheral Late/Exhausted Memory B Cells Express a Senescent-Associated Secretory Phenotype and Preferentially Utilize Metabolic Signaling Pathways." *Experimental Gerontology* 87: 113–120.

Gioia, U., S. Tavella, P. Martinez-Orellana, et al. 2023. "SARS-CoV-2 Infection Induces DNA Damage, Through CHK1 Degradation and Impaired 53BP1 Recruitment, and Cellular Senescence." *Nature Cell Biology* 25, no. 4: 550–564.

Gkioni, L., T. Nespital, M. Baghdadi, et al. 2025. "The Geroprotectors Trametinib and Rapamycin Combine Additively to Extend Mouse Healthspan and Lifespan." *Nature Aging* 5: 1249–1265.

Ha, C. W., and W. K. Huh. 2011. "Rapamycin Increases rDNA Stability by Enhancing Association of Sir2 With rDNA in Saccharomyces Cerevisiae." *Nucleic Acids Research* 39: 1336–1350.

Harrison, D. E., R. Strong, Z. D. Sharp, et al. 2009. "Rapamycin Fed Late in Life Extends Lifespan in Genetically Heterogeneous Mice." *Nature* 460: 392–395.

Hazeldine, J., P. Hampson, and J. M. Lord. 2012. "Reduced Release and Binding of Perforin at the Immunological Synapse Underlies the Age-Related Decline in Natural Killer Cell Cytotoxicity." *Aging Cell* 11: 751–759.

Hearps, A. C., G. E. Martin, T. A. Angelovich, et al. 2012. "Aging Is Associated With Chronic Innate Immune Activation and Dysregulation of Monocyte Phenotype and Function." *Aging Cell* 11: 867–875.

Houde, V. P., S. Brule, W. T. Festuccia, et al. 2010. "Chronic Rapamycin Treatment Causes Glucose Intolerance and Hyperlipidemia by Upregulating Hepatic Gluconeogenesis and Impairing Lipid Deposition in Adipose Tissue." *Diabetes* 59: 1338–1348.

Ibler, A. E. M., M. Elghazaly, K. L. Naylor, N. A. Bulgakova, and D. Humphreys. 2019. "Typhoid Toxin Exhausts the RPA Response to DNA Replication Stress Driving Senescence and Salmonella Infection." *Nature Communications* 10: 4040.

Iglesias-Bartolome, R., V. Patel, A. Cotrim, et al. 2012. "mTOR Inhibition Prevents Epithelial Stem Cell Senescence and Protects From Radiation-Induced Mucositis." *Cell Stem Cell* 11: 401–414.

Kell, L., A. K. Simon, G. Alsaleh, and L. S. Cox. 2023. "The Central Role of DNA Damage in Immunosenescence." *Frontiers in Aging* 4: 1202152.

Khadir, F., C. R. Shaler, A. Oryan, et al. 2018. "Therapeutic Control of Leishmaniasis by Inhibitors of the Mammalian Target of Rapamycin." *PLoS Neglected Tropical Diseases* 12: e0006701.

Knight, R. J., M. Villa, R. Laskey, et al. 2007. "Risk Factors for Impaired Wound Healing in Sirolimus-Treated Renal Transplant Recipients." *Clinical Transplantation* 21: 460–465.

Koufaris, C., M. Berger, and R. Aqeilan. 2025. "Causes and Consequences of T Cell DNA Damage." *Trends in Immunology* 46: 536–549.

Lee, S., Y. Yu, J. Trimpert, et al. 2021. "Virus-Induced Senescence Is a Driver and Therapeutic Target in COVID-19." *Nature* 599: 283–289.

Li, Y., Y. Shen, P. Hohensinner, et al. 2016. "Deficient Activity of the Nuclease MRE11A Induces T Cell Aging and Promotes Arthritogenic Effector Functions in Patients With Rheumatoid Arthritis." *Immunity* 45: 903–916.

Libri, V., R. I. Azevedo, S. E. Jackson, et al. 2011. "Cytomegalovirus Infection Induces the Accumulation of Short-Lived, Multifunctional CD4+CD45RA+CD27+ T Cells: The Potential Involvement of Interleukin-7 in This Process." *Immunology* 132: 326–339.

Ligotti, M. E., G. Accardi, A. Aiello, et al. 2023. "Sicilian Semi- and Supercentenarians: Identification of Age-Related T-Cell Immunophenotype to Define Longevity Trait." *Clinical and Experimental Immunology* 214: 61–78.

Lopez-Otin, C., M. A. Blasco, L. Partridge, M. Serrano, and G. Kroemer. 2023. "Hallmarks of Aging: An Expanding Universe." *Cell* 186: 243–278.

Lopez-Verges, S., J. M. Milush, S. Pandey, et al. 2010. "CD57 Defines a Functionally Distinct Population of Mature NK Cells in the Human CD56dimCD16+ NK-Cell Subset." *Blood* 116: 3865–3874.

Mannick, J. B., G. Del Giudice, M. Lattanzi, et al. 2014. "mTOR Inhibition Improves Immune Function in the Elderly." *Science Translational Medicine* 6: 268ra179.

Mannick, J. B., and D. W. Lamming. 2023. "Targeting the Biology of Aging With mTOR Inhibitors." *Nature Aging* 3: 642–660.

Mannick, J. B., M. Morris, H. P. Hockey, et al. 2018. "TORC1 Inhibition Enhances Immune Function and Reduces Infections in the Elderly." *Science Translational Medicine* 10: eaaq1564.

Mannick, J. B., G. Teo, P. Bernardo, et al. 2021. "Targeting the Biology of Ageing With mTOR Inhibitors to Improve Immune Function in Older Adults: Phase 2b and Phase 3 Randomised Trials." *Lancet Healthy Longevity* 2: e250–e262.

Markofski, M. M., J. M. Dickinson, M. J. Drummond, et al. 2015. "Effect of Age on Basal Muscle Protein Synthesis and mTORC1 Signaling in a Large Cohort of Young and Older Men and Women." *Experimental Gerontology* 65: 1–7.

Mathiasen, S. L., L. Gall-Mas, I. S. Pateras, et al. 2021. "Bacterial Genotoxins Induce T Cell Senescence." *Cell Reports* 35: 109220.

Miller, K. N., B. Li, H. R. Pierce-Hoffman, et al. 2025. "p53 Enhances DNA Repair and Suppresses Cytoplasmic Chromatin Fragments and Inflammation in Senescent Cells." *Nature Communications* 16: 2229.

Nevalainen, T., A. Autio, L. Kummola, et al. 2019. "CD27-IgD-B Cell Memory Subset Associates With Inflammation and Frailty in Elderly Individuals but Only in Males." *Immunity & Ageing* 16: 19.

Nyugen, J., S. Agrawal, S. Gollapudi, and S. Gupta. 2010. "Impaired Functions of Peripheral Blood Monocyte Subpopulations in Aged Humans." *Journal of Clinical Immunology* 30: 806–813.

Park, J. H., N. K. Lee, H. J. Lim, et al. 2020. "Pharmacological Inhibition of mTOR Attenuates Replicative Cell Senescence and Improves Cellular Function via Regulating the STAT3-PIM1 Axis in Human Cardiac Progenitor Cells." *Experimental & Molecular Medicine* 52: 615–628.

Passos, J. F., G. Saretzki, S. Ahmed, et al. 2007. "Mitochondrial Dysfunction Accounts for the Stochastic Heterogeneity in Telomere-Dependent Senescence." *PLoS Biology* 5: e110.

Riddell, N. E., S. J. Griffiths, L. Rivino, et al. 2015. "Multifunctional Cytomegalovirus (CMV)-Specific $CD8^+$ T Cells Are Not Restricted by Telomere-Related Senescence in Young or Old Adults." *Immunology* 144: 549–560.

Rolt, A., A. Nair, and L. S. Cox. 2019. "Optimisation of a Screening Platform for Determining IL-6 Inflammatory Signalling in the Senescence-Associated Secretory Phenotype (SASP)." *Biogerontology* 20: 359–371.

Saha, B., A. Cypro, G. M. Martin, and J. Oshima. 2014. "Rapamycin Decreases DNA Damage Accumulation and Enhances Cell Growth of WRN-Deficient Human Fibroblasts." *Aging Cell* 13: 573–575.

Seidler, S., H. W. Zimmermann, M. Bartneck, C. Trautwein, and F. Tacke. 2010. "Age-Dependent Alterations of Monocyte Subsets and Monocyte-Related Chemokine Pathways in Healthy Adults." *BMC Immunology* 11: 30.

Shao, L., H. Fujii, I. Colmegna, H. Oishi, J. J. Goronzy, and C. M. Weyand. 2009. "Deficiency of the DNA Repair Enzyme ATM in Rheumatoid Arthritis." *Journal of Experimental Medicine* 206: 1435–1449.

Sharp, Z. D., and R. Strong. 2023. "Rapamycin, the Only Drug That Has Been Consistently Demonstrated to Increase Mammalian Longevity. An Update." *Experimental Gerontology* 176: 112166.

Soto-Heredero, G., M. M. Gomez De Las Heras, J. I. Escrig-Larena, and M. Mittelbrunn. 2023. "Extremely Differentiated T Cell Subsets Contribute to Tissue Deterioration During Aging." *Annual Review of Immunology* 41: 181–205.

Stein, G. H., L. F. Drullinger, A. Soulard, and V. Dulic. 1999. "Differential Roles for Cyclin-Dependent Kinase Inhibitors p21 and p16 in the Mechanisms of Senescence and Differentiation in Human Fibroblasts." *Molecular and Cellular Biology* 19: 2109–2117.

Tsai, C. H., C. Y. Chang, B. Z. Lin, et al. 2021. "Up-Regulation of Cofilin-1 in Cell Senescence Associates With Morphological Change and p27(kip1) -Mediated Growth Delay." *Aging Cell* 20: e13288.

Van Deursen, J. M. 2014. "The Role of Senescent Cells in Ageing." *Nature* 509: 439–446.

Vessoni, A. T., E. C. Filippi-Chiela, C. F. Menck, and G. Lenz. 2013. "Autophagy and Genomic Integrity." *Cell Death and Differentiation* 20: 1444–1454.

Walters, H. E., and L. S. Cox. 2018. "mTORC Inhibitors as Broad-Spectrum Therapeutics for Age-Related Diseases." *International Journal of Molecular Sciences* 19: 2325.

Walters, H. E., S. Deneka-Hannemann, and L. S. Cox. 2016. "Reversal of Phenotypes of Cellular Senescence by Pan-mTOR Inhibition." *Aging (Albany NY)* 8: 231–244.

Wang, S., N. El Jurdi, B. Thyagarajan, A. Prizment, and A. H. Blaes. 2024. "Accelerated Aging in Cancer Survivors: Cellular Senescence, Frailty, and Possible Opportunities for Interventions." *International Journal of Molecular Sciences* 25: 3319.

Weichhart, T. 2018. "mTOR as Regulator of Lifespan, Aging, and Cellular Senescence: A Mini-Review." *Gerontology* 64: 127–134.

Wicke, C., A. Bachinger, S. Coerper, S. Beckert, M. B. Witte, and A. Konigsrainer. 2009. "Aging Influences Wound Healing in Patients With Chronic Lower Extremity Wounds Treated in a Specialized Wound Care Center." *Wound Repair and Regeneration* 17: 25–33.

Wilkinson, J. E., L. Burmeister, S. V. Brooks, et al. 2012. "Rapamycin Slows Aging in Mice." *Aging Cell* 11: 675–682.

Yang, Q., Q. Xi, M. Wang, et al. 2022. "Rapamycin Improves the Developmental Competence of Human Oocytes by Alleviating DNA Damage During IVM." *Human Reproduction Open* 2022: hoac050.

Yousefzadeh, M. J., R. R. Flores, Y. Zhu, et al. 2021. "An Aged Immune System Drives Senescence and Ageing of Solid Organs." *Nature* 594: 100–105.

Yousefzadeh, M., C. Henpita, R. Vyas, C. Soto-Palma, P. Robbins, and L. Niedernhofer. 2021. "DNA Damage-How and Why We Age?" *eLife* 10: e62852.

Zhang, H., G. Cicchetti, H. Onda, et al. 2003. "Loss of Tsc1/Tsc2 Activates mTOR and Disrupts PI3K-Akt Signaling Through Downregulation of PDGFR." *Journal of Clinical Investigation* 112: 1223–1233.

Zhao, J., X. Dang, P. Zhang, et al. 2018. "Insufficiency of DNA Repair Enzyme ATM Promotes Naive CD4 T-Cell Loss in Chronic Hepatitis C Virus Infection." *Cell Discovery* 4: 16.

Supporting Information

Additional supporting information can be found online in the Supporting Information section. **Figure S1:** Gating strategy for $CD4^+$ and $CD8^+$ T cells using conventional flow cytometry after in vitro T-cell-specific activation of PBMCs. **Figure S2:** Effects of mTOR inhibitors on human T cell activation over 3 days. **Figure S3:** Mitigation of DNA damage markers by rapamycin is not due to modulation of the cell cycle or protein synthesis. **Figure S4:** Flow cytometry-based measurement of autophagic flux. **Figure S5:** Autophagy is required for the resolution of DNA damage, but is not required for the mitigation of DDR upregulation by rapamycin. **Figure S6:** Gating strategy for PBMCs using 27-colour spectral flow cytometry. **Figure S7:** In vivo rapamycin treatment in older humans. **Table S1:** Details of drugs used in cell culture experiments. **Table S2:** Details of antibodies.